Human blastoids model blastocyst development and implantation.

Harunobu Kagawa[1#], Alok Javali[1#], Heidar Heidari Khoei[1#], Theresa Maria Sommer[1], Giovanni Sestini[1], Maria Novatchkova[1,2], Yvonne Scholte op Reimer[1], Gaël Castel[3], Alexandre Bruneau[3], Nina Maenhoudt[4], Jenna Lammers[3,5], Sophie Loubersac[3,5], Thomas Freour[3,5] , Hugo Vankelecom[4], Laurent David[3,6], Nicolas Rivron[1*]

# Equal contribution
* Corresponding author

1. Institute of Molecular Biotechnology of the Austrian Academy of Sciences (IMBA), Vienna BioCenter (VBC), Vienna, Austria.

2. Institute of Molecular Pathology (IMP), Vienna Biocenter (VBC), Vienna, Austria.

3. Université de Nantes, CHU Nantes, INSERM, CRTI, UMR 1064, ITUN, 44000 Nantes, France;

4. Unit of Stem Cell Research, Cluster of Stem Cell and Developmental Biology, Department of Development and Regeneration, KU Leuven, (University of Leuven), Leuven, Belgium.

5. CHU Nantes, Service de Biologie de la Reproduction, 44000 Nantes, France.

6. Université de Nantes, CHU Nantes, INSERM, CNRS, SFR Santé, FED 4203, INSERM UMS 016, CNRS UMS 3556, 44000 Nantes, France.

Abstract

Shortly after fertilization, human embryos implant into the uterus. This requires the formation of a blastocyst consisting of a sphere encircling a cavity lodging the embryo proper. Appropriate stem cells can form a blastocyst model, which we termed blastoid. Here we show that naive human pluripotent stem cells (hPSCs) triply inhibited for the Hippo, TGF-β, and ERK pathways consistently and efficiently (>70%) form blastoids that generate transcriptional pre-implantation analogs of the three founding lineages (trophoblast, epiblast, primitive endoderm; >97%) according to the sequence and pace of blastocyst development. Blastoids spontaneously form an axis marked by the maturation of the polar region, which acquires the potential to specifically attach to hormonally stimulated endometrial cells, as during *in utero* implantation. Such human blastoids are scalable, versatile, and ethical models to explore human implantation and development.

Introduction.
A high-fidelity and high-efficiency model of the human blastocyst would support scientific and medical progress[1]. Its capacity to predict events of human development will depend on its ability to efficiently and faithfully recapitulate the sequences of blastocyst cellular specification and morphogenesis, according to the developmental pace. Faithful modeling would ensure the formation of cells reflecting the blastocyst stage only as well as an accurate recapitulation of aspects of blastocyst and peri-implantation development *in vitro*.

Triply inhibited (Hippo/ERK/TGF) naive hPSCs form blastocyst-like structures efficiently and timely. The blastocyst forms within 3-4 days, while generating 3 founding lineages that form the whole conceptus: the epiblast (EPI, embryonic), trophectoderm (TE, extraembryonic) and primitive endoderm (PrE, extraembryonic)(**Fig. 1A**). In the embryo, peripheral cells become TE by inhibiting the Hippo pathway[2]. Also, naive hPSCs (cultured in PXGL[3]) efficiently form TE upon inhibition of TGF-β and ERK pathways[4–8]. Therefore, we formed clusters of naive hPSCs in non-adherent hydrogel microwells[9] and inhibited these three pathways (one-step protocol, **Fig. 1B & Sup. Fig. 1A-C**). Upon exposure to Lysophosphatidic Acid (LPA, Hippo pathway inhibitor[10]), A83-01 (TGF-β family receptors inhibitor) and PD0325901 (ERK inhibitor) in a chemically-defined medium containing LIF (STAT activator) and Y-27632 (ROCK inhibitor), blastocyst-like structures formed efficiently (>70% of microwells, **Fig. 1C-E & Sup. video 1,** 150 < diameter < 200 um, see full morphometric criteria in *Methods*)**,** and consistently (>20 passages, **Sup. Fig. 1D**). LPA was essential for efficiency (**Sup. Fig. 1B-D**). Within 5 days the cell number ($47^{+/-}9$ to $129^{+/-}27$) and overall size (65 to 200 µm) increased (**Sup. Fig. 1E, F**) as in the range of day 5-7 blastocysts (morphological stages B3-6)[11,12]. TE cells analogs ($GATA2^+/GATA3^+/CDX2^+/TROP2^+$)[12,13] formed and proliferated (**Fig. 1F-H & Sup. Fig. 1G-L**), established adherens junctions (Epithelial cadherin (CDH1)), apical-basal polarity (aPKC localization) and tight junctions ($ZO\text{-}1^+$ **Fig. 1I** and **Sup. Fig. 1M**) while undergoing cycles of inflations/deflations (**Sup. Fig. 1N and Sup. video 2**)[14]. Surprisingly, all blastocyst-like structures set apart a unique cluster of inner cells reflecting the EPI ($OCT4^+$; average = $27^{+/-}13$ cells; 26% of total cells) and PrE ($GATA4^+/SOX17^+/PDGFRa^+$ average = $7^{+/-}5$ cells; 7% of total cells)(**Fig. 1F-H & Sup. Fig. 1H, I, L**). Multiple lines of naive hESCs (Shef6, H9, HNES1) and hiPSCs (niPSC 16.2.b, cR-NCRM2) formed such structures with comparable high efficiency (**Fig. 1E & Sup. Fig. 1O**), while primed hPSCs that reflect the post-implantation EPI[15] did not (**Sup. Fig. 1P**).

Blastocyst-like structures are composed of analogs of the three pre-implantation lineages. Single cell transcriptomics analysis showed that, overtime, blastocyst-like structures formed three main transcriptomic states (**Fig. 2A-C & Sup. Fig. 2A**) marked by genes specific to the three founding lineages, including *GATA2/GATA3* (TE), *POU5F1*/*KLF17* (EPI), and *GATA4*/*SOX17* (PrE)(**Fig. 2C, D & Sup. Fig. 2B**). Comparison with cells from blastocysts[16], *in vitro* cultured blastocysts[17] and a gastrulation-stage embryo[18] disclosed that cells were transcriptionally similar to pre-implantation state and distinct from post-implantation ones (**Fig. 2E, F** & **Sup. Fig. 2C-H**). A higher-resolution clustering (x50) of single cells isolated one cluster of non-blastocyst-like cells with a gene expression pattern reminiscent of post-implantation tissues (*GABRP*, *ISL1*, *APLNR*, *CRABP2*)[19](**Sup. Fig. 2I-K**) and which appeared transcriptionally similar to post-implantation amnion (annotated as non-neural-ectoderm[18]) and mesoderm (**Sup. Fig. 2L-Q**). Of note, these non-blastocyst-like

cells constituted less than 3% of the cells composing the blastocyst-like structure, which is less than the differentiated cells residing in naive hPSCs culture (5,6%, **Sup. Fig. 2P**)[20]. Bulk RNA sequencing analysis also revealed that isolated trophoblast analogs (TROP2$^+$, by flow cytometry) had an intermediate transcriptome between naive hPSCs and previously established post-implantation-like trophoblasts (hTSCs)[21,22] (**Sup. Fig. 3A**). Furthermore, they were enriched in TE transcripts (Blastocyst-stage: *ESRRB*, *GRHL1*, *OVOL1*, *GATA2, GATA3*, *TBX3*, *KRT19*) but not in post-implantation markers (*CGB5, CGB7*, *SIGLEC6*, *CGA*, *DPP4* **Sup. Fig. 3B**). The transcriptome of isolated EPI analogs (TROP2$^-$/PDGFRa$^-$) resembled the one of naive hPSCs (**Sup. Fig. 3A**). It was enriched in markers specific for blastocyst-stage EPI (*KLF17*, *ATG2A*, *SUSD2*, *TFCP2L1*, *ZFP57*, *DPPA2*, *UTF1*, *PRDM14*)[23,24] and differed from the transcriptome of primed hPSCs (**Sup. Fig. 3C**). Finally, isolated PrE analogs (PDGFRa$^+$) had an intermediate transcriptome between naive hPSCs and previously established extraembryonic endoderm cell lines (nEND cells)[25](**Sup. Fig. 3A**). Cells were enriched in blastocyst-stage PrE markers[24] (*Early blastocyst*: *GATA6*, *MSX2*, *HNF4A*. *Late blastocyst*: *PDGFRA*, *GATA4*, *SOX17*, *HNF1B*, *FOXA2*) and downregulated EPI genes (*ARGFX*, *PRDM14*, *SOX2*, *NANOG*, *DPPA2*, *POU5F1*), as previously described in blastocysts(**Sup. Fig. 3D**)[24]. EPI genes were further downregulated in nEND cells. Overall, these blastocyst-like structures are composed of three cell types transcriptionally similar to the pre-implantation stage. Blastocysts have the ability to establish stem cell lines. Blastocyst-like structures permitted *de novo* derivation of naive hPSCs (NANOG$^+$/SOX2$^+$/OCT4$^+$/KLF17$^+$)[26] (**Sup. Fig. 4A**) able to form 2nd generation blastocyst-like structures (**Sup. Fig. 4B, C**) and hTSCs (CDX2$^-$/GATA3$^+$/CK7$^+$)[21] (**Sup. Fig. 4D**) endowed with rapid differentiation capacity into syncytio- and extravillous trophoblast tissues (SCT and EVT respectively) (3-6 days, **Sup. Fig. 4E-J**). Of note, derivation of PrE cell lines from human blastocysts has not been reported. Altogether, because these blastocyst-like structures self-organized three cell states (97%) transcriptionally similar to the pre-implantation lineages in the sequential and timely manner of blastocyst development, we refer to these models as blastoids[27].

Hippo pathway inhibition is essential for blastoid formation. Knowledge about the first lineage segregation and progression in human embryos is limited to a handful of gene expression changes (**Fig. 3A**). One well studied mechanism is the Hippo pathway, whose inhibition occurs upon acquisition of an apical domain in the peripheral cells and eventually leads to the acquisition of trophoblast fate (**Sup. Fig. 5A**)[28,29]. We tested the co-option of this mechanism during blastoid formation. Strikingly, atypical Protein Kinase C (aPKC) and F-actin expression domains appeared co-aligned in outer cells that also accumulated Hippo downstream effector YAP1 in nuclei (**Fig. 3B & Sup. Fig. 5B**). YAP1 nuclear location correlated with GATA2/3 expression[30], contrasted with NANOG expression and became restricted to the TE analogs (**Fig. 3B & Sup. Fig. 5C**). An aPKC inhibitor (CRT0103390)[30] largely prevented YAP1 nuclear accumulation, decreased the number of GATA3$^+$ cells and prevented blastoid formation (**Fig. 3C & Sup. Fig. 5D, E**). *Per contra*, ligands of the LPA receptors (LPA and NAEPA) that inhibit the Hippo pathway[10] enhanced blastoid formation (**Fig. 3D & Sup. Fig. 5F**). Because Hippo pathway inhibition frees YAP1 to enter the nucleus, we tested whether genetically engineered levels and functions of YAP1 impacted morphogenesis. Over-expression of wildtype or constitutively active forms of YAP1 (5SA)[31] accelerated cavitation (**Fig. 3E**). The interaction between YAP1 and TEAD transcription factors is necessary for the down-stream gene regulation[32]. Accordingly, over-expression of YAP1 comprising a mutation in the TEAD binding site (S94A) did not impact cavitation (**Fig.**

3E & Sup. Fig. 5G). Verteporfin, a drug that disrupts the YAP1-TEAD interaction[33], prevented blastoid formation (**Fig. 3F**). Cavity morphogenesis occurred through the apparent coalescence of multiple fluid-filled cavities (60 hours, yellow arrows in **Sup. Fig. 5H**)[34]. Aquaporin 3 (AQP3), the water transporter most highly expressed in human blastocysts[23], was initially visible in all cells (36 hours) and then restricted to the TE analogs (96 hours) (**Sup. Fig. 5I**). Thus, similar to blastocysts in humans and other species[30], trophoblast specification and morphogenesis in blastoids depends on aPKC, inhibition of the Hippo pathway, nuclear translocation of YAP1 and its ability to bind TEAD transcription factors.

The three lineages progress according to the sequence of blastocyst development.
In blastocysts, the trophoblast lineage appears first (days 5-6, $GATA2^+/DAB2^+$)[23,24] and the PrE lineage second (days 6-7, $GATA6^+/ADM^+$)[24]. In blastoids, the sequential lineage specification is recapitulated with trophoblasts forming first (< 24 hours)[23,24] expressing early and general TE genes *DAB2*[24], *CDX2,* and *GATA2/3* (**Fig. 3G, H**). Concomitantly, they changed transcript levels related to PKC and Hippo signaling (*AKAP12, CAPZB, ULK4, MOB1a, AMOT, AMOTL2, LATS2, TEAD1*)(**Extended table 1**). At protein level, these early TE-like cells first appeared $YAP1^{nuclear}/GATA2^+$ (24 hours), then $CDX2^+/GATA3^+$ while maintaining KLF17/OCT4 but not NANOG (60 hours) (**Fig. 3B, I & Sup. Fig. 6A-C**). Subsequently, OCT4 became undetectable (**Fig. 1G & Sup. Fig. 1K**)[12,23]. SMAD, ERK, Notch, and Wnt signaling pathway associated genes were regulated during the progression (**Sup. Fig. 6D,E; Extended table 1)** Finally, polar-like trophoblasts matured as marked by expression of *OVOL1, GREM2*, *CCR7, SP6,* and *NR2F2* (**Fig. 3H & Sup. Fig. 6F**), up-regulation of NR2F2[23] and CCR7[16], and down-regulation of CDX2 (**Fig. 3J & Sup. Fig. 6G, H**). The transcriptome of EPI analogs maintained the core markers of the blastocyst EPI (*POU5F1, NANOG, KLF17, SUSD2, KLF4, ARGFX, GDF3*)(**Fig. 3K & Sup. Fig. 6I, J; Extended table 1**), while undergoing an overtime evolution characterized by downregulation of Nodal signaling-related genes (*NODAL, LEFTY1/2*), upregulation genes related to mTOR signaling (*LAMTOR1/4/5, XBP1, SEC13, MLST8*) and of the X chromosome activation-related gene *XACT* (**Sup. Fig. 6K)**. Finally, PrE analogs appeared within 60 hours, and GATA4, OTX2, and SOX17 were detected at 72 hours (**Fig. 3G & Sup Fig. 6L-N**[23]). Early PrE marker genes (*GATA6*, *LBH*, *ADM*, and *LAMA1*)[24] were uniformly expressed among the PrE analog cells, while some late PrE marker genes (CTSE, APOA1, PITX2 and SLCO2A1) were only expressed in a subpopulation. This suggests that the PrE analogs are undergoing a developmental progression from an early to late PrE state (**Fig. 3L**)[23]. Mature PrE (96 hours) had regulated SMAD (*NODAL, BMP2/6, GDF3, ID1/2*) and Wnt signaling related transcripts (*WNT3, RSPO3*, *LBH*), and enriched in transcripts controlling extracellular matrix organization (*LAMA1/5, LAMB1, LAMC1, COL4A1/2*), endodermal and epithelial differentiation (**Fig. 3L & Sup. Fig. 6O**).

Human blastoids interact specifically with endometrial cells made receptive.
Human blastocysts implant *in utero* on days 7-9. This process starts by the apposition and attachment of the TE to the endometrium (**Fig. 4A, left**), a process that requires the active interaction of a matured polar TE and a receptive endometrium[35,36]. We thus wondered whether blastoids could model this interaction. First, we seeded endometrial organoids[37] in 2D to form an open-faced endometrial layer (OFEL) facilitating blastoid deposition (**Fig. 4A, right**). Subpopulations of OFELs were positive for acetylated alpha tubulin marking ciliated epithelial cells (**Sup. Fig. 7A**)[37] and FOXA2 marking glandular epithelial cells (**Sup. Fig.**

7B)[38], suggesting presence of both ciliated and unciliated endometrial epithelial cells that form the uterus lining. *In utero*, the window of implantation opens upon estrogen (E2) and progesterone (P4) exposure along with Wnt inhibition[39,40]. Accordingly, OFELs responded to E2, P4, cAMP and XAV939 by upregulating the expression of genes that mark the mid-secretory phase endometrium (**Sup. Fig. 7C-E**)[41] along with decreasing proliferation[40] (**Sup. Fig. 7E, F**). Interestingly, human blastoids deposited onto non-stimulated OFELs did not attach. On the contrary, blastoids interacted with stimulated OFELs by attaching to and then repulsing[42] endometrial cells as occurring *in vivo* (**Fig. 4B & Sup. Fig. 7G, H**). The contraceptive Levonorgestrel[43] impaired blastoid attachment (**Sup. Fig. 7I**). We concluded that human blastoids are competent for interaction with an endometrium made receptive.

Epiblast induces polar trophoblast maturation to gatekeep endometrium interactions. Human blastocyst attach to the endometrium *via* the polar region, which is defined by its physical contact with the EPI[39]. Similarly, blastoids initiated attachment *via* the polar region[39] (**Fig 4 C, D & Sup. Fig. 8A & Sup video 3**). We thus tested the importance of the polar/EPI communication by forming trophospheres devoid of EPI, in two different ways. IL6 is highly expressed in the polar TE and transcripts for its receptor (*IL6R*, *GP130*) and effector (*STAT3*) abound in EPI (**Sup. Fig. 8B**). Consistent with a role for STAT signaling in EPI, blastoid formation efficiency increased with LIF concentration (**Sup. Fig. 8C**) while the addition of a GP130 inhibitor (SC144[44]) yielded trophospheres (**Fig. 4E & Sup. Fig. 8D**). The presence of a potent inhibitor of the Hippo kinases MST1/2 (XMU-MP-1[45]) also yielded trophospheres (**Fig. 4E & Sup. Fig. 8E**). The transcriptome of these trophospheres reflected early and late blastocyst trophoblasts, respectively **(Sup. Fig. 8F, G)**. Both types of trophospheres failed to attach to OFELs made receptive (**Fig. 4E**), so did aggregates of hTSCs[21] that reflect post-implantation cytotrophoblasts ($CDX2^-/CK7^+$, **Fig. 4 E, F & Sup. Fig. 8F-H**)[4]. Thus signals from the EPI ensure maturation of the polar trophoblast, which is important to interact with the endometrial cells. Based on transcriptome analysis and data from *in utero* cells[40], we propose several pairs of molecules whose transcripts became more abundant upon stimulation of endometrial cells and whose ligand was expressed upon maturation of the polar trophoblast analogs (**Sup. Fig. 8I**). These pairs might mediate the first communication and attachment between the blastocyst and the uterus. Overall, we concluded that a pre-implantation polar-like state whose maturation is dependent on EPI inductions, gate-keeps interactions with the endometrium.

Human blastoids model aspects of peri-implantation development until day 13. Upon extending blastoid culture in peri-implantation conditions[43,44], blastoid morphology was stable for two days (despite increased osmolarity, **Sup. Fig. 9A**)[46,47] and, once attached on OFEL or on Matrigel, cells progressed according to some features of blastocyst development. Clinical pregnancy is characterized by the detection of Chorionic Gonadotropin β (CGβ) hormone. Upon attachment, blastoids formed trophoblasts expressing CGβ at levels detectable using standard pregnancy tests and ELISA (**Fig. 4G, H & Sup. Fig. 9B**). $NR2F2^+$ polar trophoblast analogs proliferated and the majority of trophoblasts no longer expressed CDX2 while upregulating the peri-implantation gene Cytokeratin 7 (CK7) (**Sup. Fig. 9C, D**). Upon prolonged culture, lineages consistently expanded **(Sup. Fig. 9E)**. Trophoblasts further differentiated into SCT and EVT expressing CGβ and HLA-G respectively **(Sup. Fig. 9F, G)**. EPI analogs maintained OCT4, SOX2, upregulated primed pluripotency marker CD24 **(Fig. 4I & Sup. Fig. 9D, H)**[48]; accumulation of cortical F-actin recapitulated aspects of EPI

epithelization , and some blastoids formed pro-amniotic-like cavities enriched with F-actin/PODXL^{+}/aPKC^{+} **(Fig. 4I & Sup. Fig. 9I).** Also, a subpopulation in the periphery of the EPI analog expressed CDX2 along with SOX2 or TFAP2C, suggestive of an early amnion-like state **(Sup. Fig. 9J, K)**[49]. PrE analogs were characterized by their restricted expression of OTX2 (**Fig. 3M & Sup. Fig. 9L**)[23]. The three lineages had consistently expanded 6 days after the blastocyst-like stage (time-equivalent of day 13)**(Fig 4J)**. Although, similar to cultured blastocysts, their organization did not reflect that developmental stage.

Discussion. The fidelity, scalability, and versatility of this model makes it relevant for the study of human blastocyst development and implantation. It may aid to improve IVF media formulation, identify therapeutic targets and contribute to preclinical modeling (*e.g.* contraceptives such as candidate SC144)[1]. Considering the proportionality (balancing the benefits and harms) and subsidiarity (pursuing goals using the morally least problematic means) of human embryology, human blastoids represent an ethical opportunity complementing research using human embryos[50].

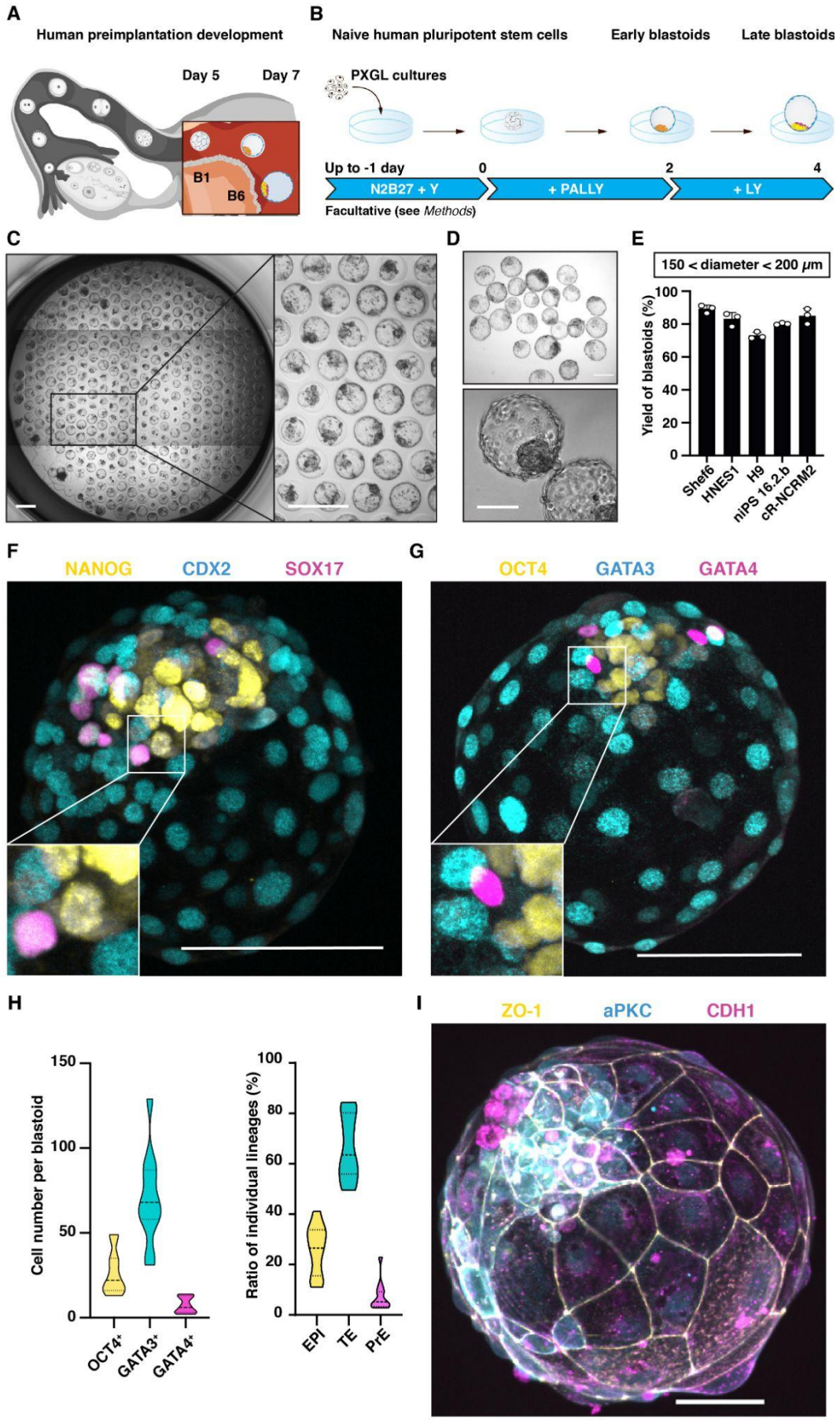
A
Human preimplantation development
Day 5
Day 7
B1
B6
B
Naive human pluripotent stem cells
Early blastoids
Late blastoids
PXGL cultures
Up to -1 day
0
2
4
N2B27 + Y
+ PALLY
+ LY
Facultative (see Methods)
C
D
E
150 < diameter < 200 μm
Yield of blastoids (%)
100
80
60
40
20
0
Shef6
HNES1
H9
niPS 16.2.b
cR-NCRM2
F
NANOG
CDX2
SOX17
G
OCT4
GATA3
GATA4
H
Cell number per blastoid
150
100
50
0
OCT4+
GATA3+
GATA4+
Ratio of individual lineages (%)
100
80
60
40
20
0
EPI
TE
PrE
I
ZO-1
aPKC
CDH1

Figure 1: Triply inhibited naive hPSCs efficiently form human blastocyst-like structures comprising analogs of the three founding lineages. A. A schematic of the time window of human peri-implantation development hereby modeled. B1 and B6 indicate the range of blastocyst developmental stages[51]. **B.** One-step protocol of human blastoid formation. N2B27: serum-free medium. PALLY: **P**D0325901, **A**83-01, h**L**IF, **L**PA, **Y**-27632. **C.** Human blastocyst-like structures formed on a non-adherent hydrogel microwell array after 96 hours. Each microwell is 200 μm in diameter. Scale bars: 400 μm. **D.** Phase-contrast image of representative human blastocyst-like structures harvested from microwells. Scale bars: 200 μm (**top**) and 100 μm (**bottom**). **E.** Quantification of the percentage of microwells including a human blastocyst-like structure for different naive hPSC lines cultured in PALLY condition with optimized LPA concentration (yield of blastocyst-like structures (%); also see morphometric definition of a blastocyst-like structures in *Methods*. n=3 microwell arrays). Error bar: S.D. **F, G.** Immunofluorescence stainings for the epiblast (EPI) markers (Yellow) NANOG (**F**) and OCT4 (**G**); the TE markers (Cyan) CDX2 (**F**) and GATA3 (**G**); and the primitive endoderm marker (Magenta) SOX17 (**F**) and GATA4 (**G**) in human blastocyst-like structures. Scale bar: 100 μm. **H.** Quantification of the absolute number of cells positive for OCT4, GATA3 and GATA4 (**left**) and of the ratios of cells belonging to individual lineages represented as percentage of total number of cells (**right**) in blastocyst-like structures (96 hours) based on immunofluorescence stainings. **I**. Representative immunofluorescence stainings for the tight junction molecule ZO-1 (Yellow), the adherence junction molecule CDH1 (Magenta), and the apical domain molecule aPKC (Cyan) in a representative human blastocyst-like structure. Scale bars: 50 μm.

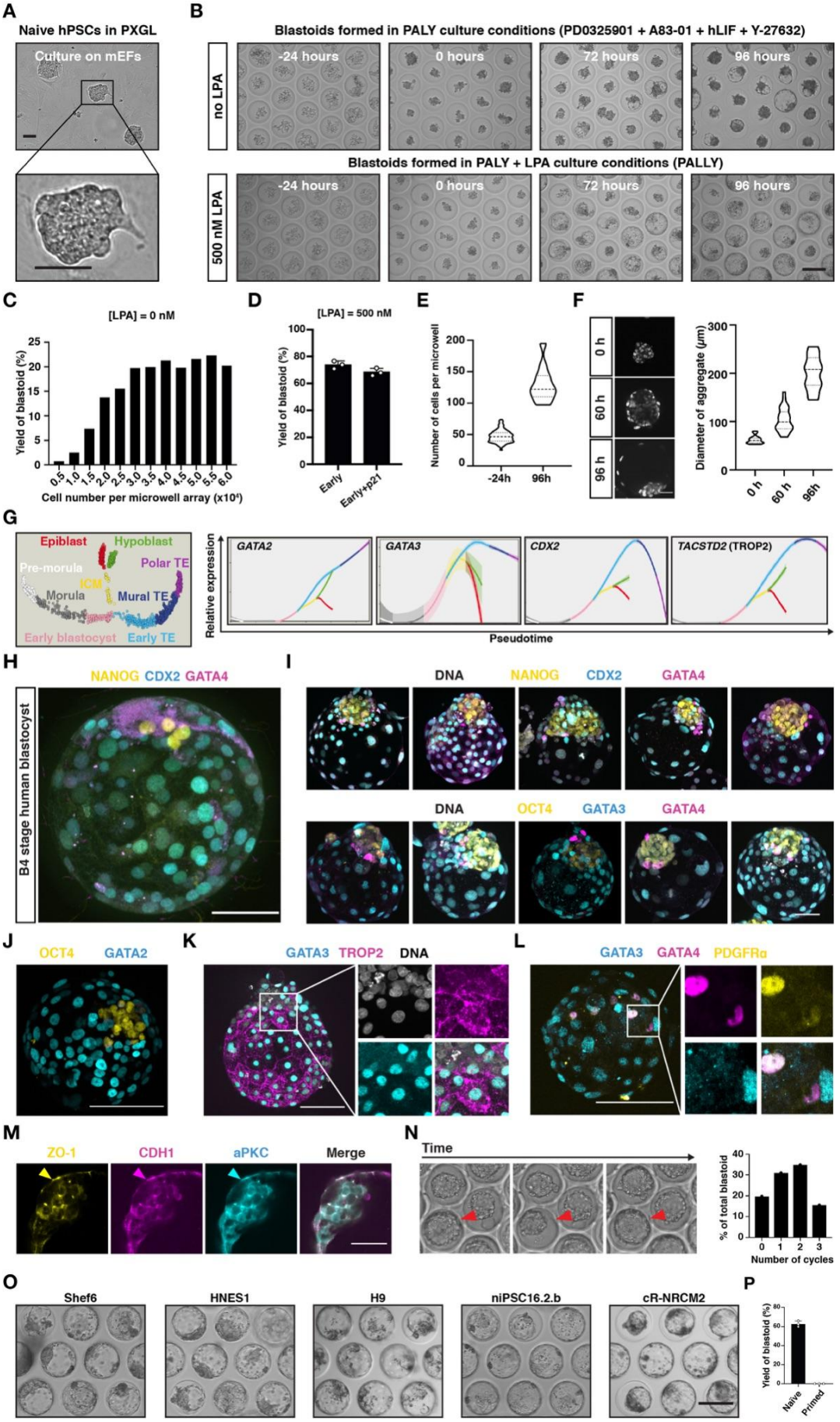
A
Naive hPSCs in PXGL
Culture on mEFs
B
Blastoids formed in PALY culture conditions (PD0325901 + A83-01 + hLIF + Y-27632)
no LPA
-24 hours
0 hours
72 hours
96 hours
Blastoids formed in PALY + LPA culture conditions (PALLY)
500 nM LPA
-24 hours
0 hours
72 hours
96 hours
C
[LPA] = 0 nM
Yield of blastoid (%)
Cell number per microwell array (x10⁴)
D
[LPA] = 500 nM
Yield of blastoid (%)
Early
Early+p21
E
Number of cells per microwell
-24h
96h
F
0 h
60 h
96 h
Diameter of aggregate (μm)
0 h
60 h
96h
G
Epiblast
Hypoblast
Polar TE
Pre-morula
ICM
Morula
Mural TE
Early blastocyst
Early TE
Relative expression
GATA2
GATA3
CDX2
TACSTD2 (TROP2)
Pseudotime
H
NANOG CDX2 GATA4
B4 stage human blastocyst
I
DNA NANOG CDX2 GATA4
DNA OCT4 GATA3 GATA4
J
OCT4 GATA2
K
GATA3 TROP2 DNA
L
GATA3 GATA4 PDGFRα
M
ZO-1
CDH1
aPKC
Merge
N
Time
% of total blastoid
Number of cycles
O
Shef6
HNES1
H9
niPSC16.2.b
cR-NRCM2
P
Yield of blastoid (%)
Naive
Primed

Figure S1: Naive hPSCs form human blastocyst-like structures comprising analogs of the three founding lineages. A. Phase contrast images of naive hPSCs cultured in PXGL medium and on MEF feeder layers. Scale bar: 50 µm. **B.** Time course phase contrast images of naive hPSCs aggregates cultured within microwell arrays either without LPA (PALY medium, **top**) or with 500 nM LPA (PALLY medium, **bottom**). Scale bar: 200 µm. **C.** Quantification of the effect of the initial cell numbers per microwell array on the yield of blastocyst-like structures. n=1 microwell arrays. **D.** Quantification of the effect of serial passaging of naive hPSCs on the yield of blastocyst-like structures. n=3 microwell arrays. Error bar: S.D. **E.** Quantification of the cell numbers per microwell at the time of seeding and in blastocyst-like structures at 96 hours when cells are seeded at 3.0 x 10^4 cells per microwell array. n=200 microwells (24 hrs.) and n=12 blastocyst-like structures (96 hrs.). **F.** Fluorescence staining of DNA using Hoechst in representative naive hPSCs aggregates over the course of formation of blastocyst-like structures (96 hours, **left**). Measurement of the distributed diameters of the structures over the course of formation of blastocyst-like structures (**right**). n=15, 31 and 11 for 0, 60 and 96 hours, respectively. Scale bar: 50 µm. **G.** Pseudotime analysis of human pre-implantation development showing the expression of the TE markers *GATA2, GATA3, CDX2 and TACSTD2*. Gene expression analysis was performed by using the public data analysis tool (https://bird2cluster.univ-nantes.fr/demo/PseudoTimeUI/). **H.** Immunofluorescence stainings for EPI marker NANOG (Yellow), TE marker CDX2 (Cyan) and primitive endoderm marker GATA4 (Magenta) in a representative B4-stage human blastocyst. Scale bar: 50 µm. **I.** Immunofluorescence stainings for the EPI markers (Yellow) NANOG (**top**) and OCT4 (**bottom**); the TE markers (Cyan) CDX2 (**top**) and GATA3 (**bottom**); and the primitive endoderm marker (Magenta) GATA4 in five representative blastocyst-like structures. Counterstain with Hoechst (Grey) marking DNA. Scale bar: 50 µm. **J.** Immunofluorescence staining for EPI marker OCT4 (yellow) and TE marker GATA2 (Cyan) in blastocyst-like structures. **K.** Immunofluorescence staining for TE markers GATA3 (Cyan) and TROP2 (Magenta) in blastocyst-like structures. **L.** Immunofluorescence staining for TE markers GATA3 (Cyan) and GATA4 (Magenta) and the PrE marker PDGFRa (Yellow) in blastocyst-like structures. **M.** Single optical section of immunofluorescence staining image for the tight junction molecule ZO-1 (Yellow), the adherence junction molecule CDH1 (Magenta), and the apical domain molecule aPKC (Cyan) in a representative human blastocyst-like structures. Scale bars: 50 µm. **N.** Representative time points from a timelapse image of naive cell aggregates, cavitating into blastocyst-like structures while showing cycles of cavity inflation and deflation (**left**) - quantification of blastocyst-like structures showing distinct frequencies of inflation and deflation (**right**). **O.** Phase contrast images of representative areas of microwell arrays showing blastocyst-like structures formed from different naive hPSCs and hiPSCs lines. **P.** Quantification of the yield of blastocyst-like structures obtained from naive and primed H9 hPSCs. n=3 microwell arrays. Error bar: S.D.

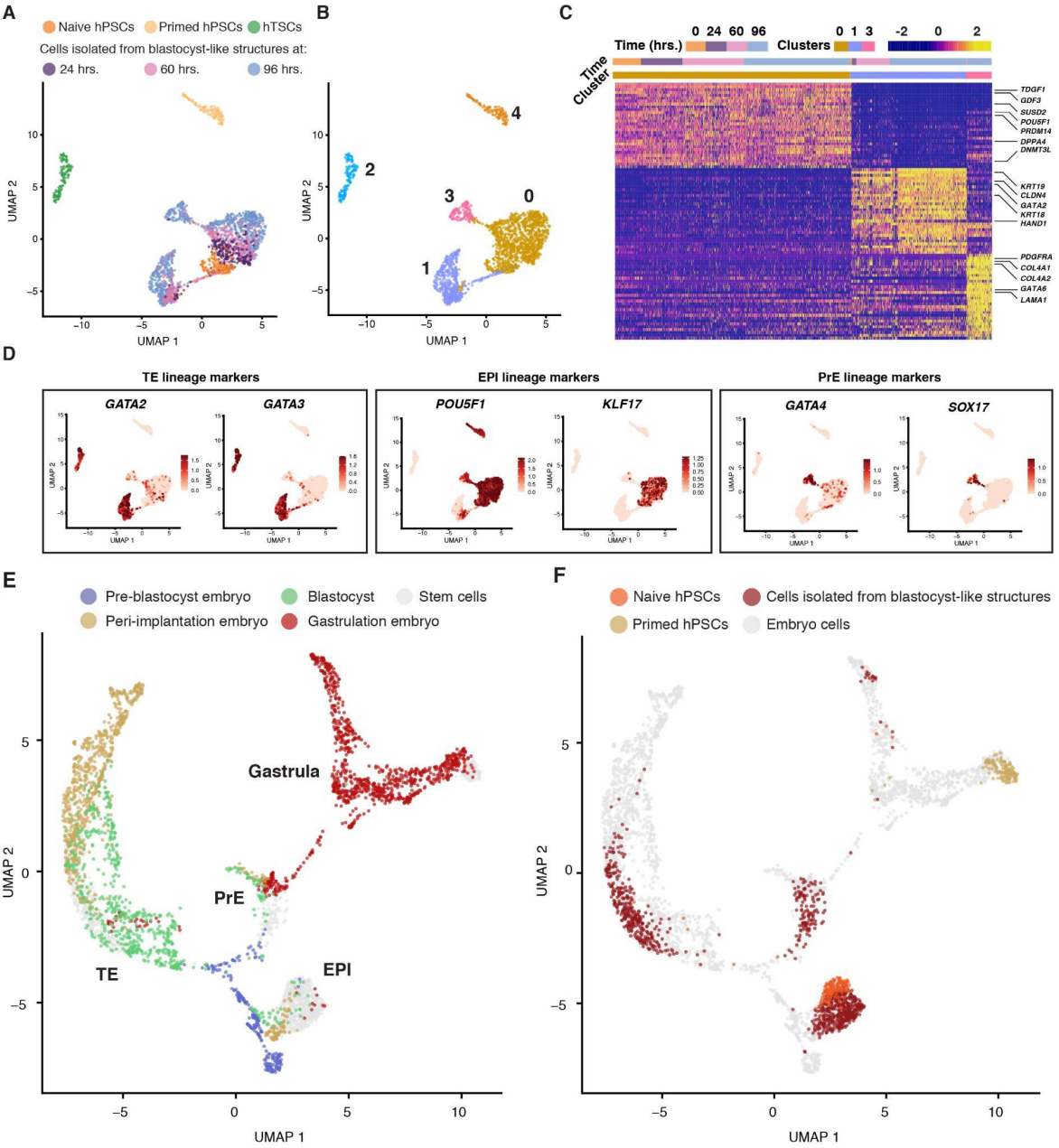
A
Naive hPSCs
Primed hPSCs
hTSCs
Cells isolated from blastocyst-like structures at:
24 hrs.
60 hrs.
96 hrs.
UMAP 2
UMAP 1
B
4
2
3
0
1
C
Time (hrs.)
0 24 60 96
Clusters
0 1 3
-2 0 2
Time
Cluster
TDGF1
GDF3
SUSD2
POU5F1
PRDM14
DPPA4
DNMT3L
KRT19
CLDN4
GATA2
KRT18
HAND1
PDGFRA
COL4A1
COL4A2
GATA6
LAMA1
D
TE lineage markers
GATA2
GATA3
EPI lineage markers
POU5F1
KLF17
PrE lineage markers
GATA4
SOX17
E
Pre-blastocyst embryo
Blastocyst
Stem cells
Peri-implantation embryo
Gastrulation embryo
Gastrula
PrE
TE
EPI
UMAP 2
UMAP 1
F
Naive hPSCs
Cells isolated from blastocyst-like structures
Primed hPSCs
Embryo cells
UMAP 2
UMAP 1

Figure 2: Human blastocyst-like structures form analogs of the three pre-implantation lineages. A, B. UMAP of the transcriptome of single cells originating from blastocyst-like structures (24, 60, 96 hours), naive hPSCs, primed hPSCs and hTSC (represent the post-implantation cytotrophoblast); individual cells are colored based on their origin (**A**) or their unsupervised cluster affiliation (**B**). **C.** Unsupervised distance map generated using top 30 genes that are enriched in clusters 0, 1 and 3 (defined in the UMAP (see **B**)). **D.** Expression level of genes specific to each blastocyst lineage (trophectoderm (TE), epiblast (EPI) and primitive endoderm (PrE)). **E,F.** UMAP of single cell transcriptome of cells from blastocyst-like structures, naive hPSCs and primed hPSCs integrated with published data sets from human embryos of pre-implantation[16], peri-implantation (*in vitro* cultured blastocysts)[17] and gastrulation (Carnegie stage 7, i.e., between E16-19) stages[18]. Individual cells are colored based on their origin in human embryos (**E**), blastocyst-like structures or stem cells (**F**).

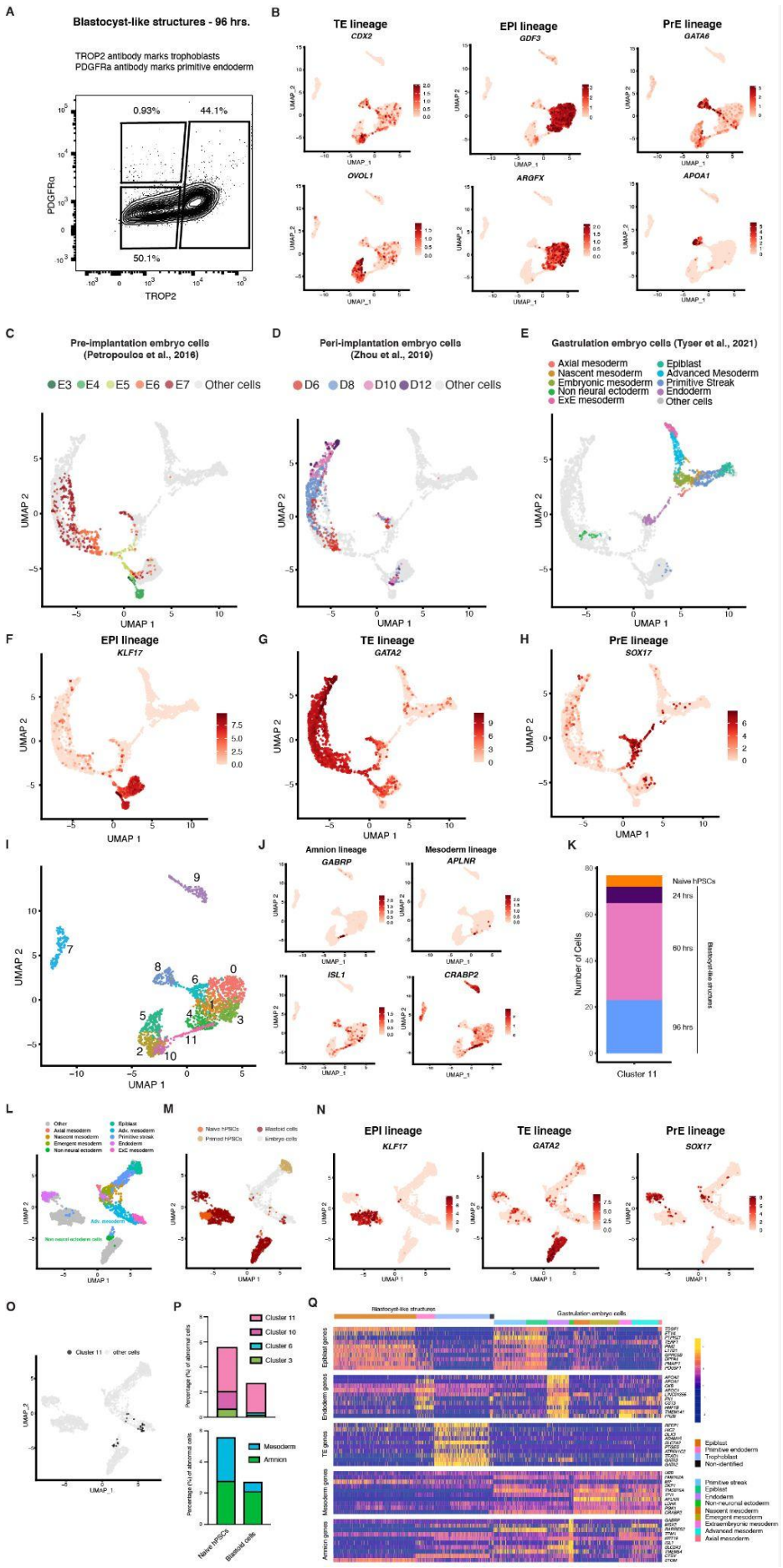
A
Blastocyst-like structures - 96 hrs.
TROP2 antibody marks trophoblasts
PDGFRa antibody marks primitive endoderm
0.93%
44.1%
50.1%
PDGFRα
TROP2
B
TE lineage
CDX2
EPI lineage
GDF3
PrE lineage
GATA6
OVOL1
ARGFX
APOA1
C
Pre-implantation embryo cells (Petropoulos et al., 2016)
E3 E4 E5 E6 E7 Other cells
D
Peri-implantation embryo cells (Zhou et al., 2019)
D6 D8 D10 D12 Other cells
E
Gastrulation embryo cells (Tyser et al., 2021)
Axial mesoderm
Nascent mesoderm
Embryonic mesoderm
Non rieural ectoderm
EXE mesoderm
Epiblast
Advanced Mesoderm
Primitive Streak
Endoderm
Other cells
F
EPI lineage
KLF17
G
TE lineage
GATA2
H
PrE lineage
SOX17
UMAP 1
UMAP 2
I
J
Amnion lineage
GABRP
Mesoderm lineage
APLNR
ISL1
CRABP2
K
Naive hPSCs
24 hrs
60 hrs
96 hrs
Blastocyst-like structures
Number of Cells
Cluster 11
L
M
N
EPI lineage
KLF17
TE lineage
GATA2
PrE lineage
SOX17
O
Cluster 11
other cells
P
Cluster 11
Cluster 10
Cluster 6
Cluster 3
Percentage (%) of abnormal cells
Mesoderm
Amnion
Naive hPSCs
Blastoid cells
Q
Blastocyst-like structures
Gastrulation embryo cells
Epiblast genes
Endoderm genes
TE genes
Mesoderm genes
Amnion genes
Epiblast
Primitive endoderm
Trophoblast
Non-identified
Primitive streak
Epiblast
Endoderm
Non-neuronal ectoderm
Nascent mesoderm
Emergent mesoderm
Extraembryonic mesoderm
Advanced mesoderm
Axial mesoderm

S2. Human blastocyst-like structures form analogs of pre-implantation lineages. A. Flow cytometry analysis plot of cells isolated from blastocyst-like structures and stained for lineage-specific surface markers PDGFRa (PrE) and TROP2 (TE). The gates were used to sort analogs of EPI (double negative), TE (TROP2^{high}) and PrE (PDGFRα^{high}) to subsequently process for single cell RNA sequencing. Note that the gates did not exclude any cells. This analysis was performed to correlate protein and RNA measures, while ensuring a representation of all cell types. **B.** UMAPs of the transcriptome of single cells isolated from blastocyst-like structures and displaying the expression levels of genes specific for each of the three blastocyst lineages (TE - Trophectoderm, EPI - Epiblast, and PrE- Primitive endoderm). **C-E.** UMAPs of single cells isolated from both blastocyst-like structures and from embryos ranging from E3 to E19. **C.** Coloration of cells originating from *In Vitro Fertilization* (IVF) embryos isolated on day 3 (E3) to day 7 (E7). This period comprises only pre-implantation stage embryos. **D.** Coloration of cells originating from IVF embryos isolated on day 6 (E6) to day 12 (E12). These blastocysts (E6) were cultured *in vitro*. Note that this annotation reflects the number of days in culture rather than the developmental stages. **E.** UMAP of the transcriptome of cells isolated from blastocyst-like structures and gastrulation-stage embryos with coloration of cells originating from embryos isolated on day 17 (E17) to 19 (E19). **F-H.** UMAPs of single cells isolated from both blastocyst-like structures and from embryos ranging from E3 to E19 and displaying the expression levels of genes specific for each of the three blastocyst lineages (EPI, TE, and PrE). **I.** UMAP of clusters formed from cells isolated from blastocyst-like structures (high-resolution clustering of 1, x50 as compared to **Fig. 2B**). **K.** Origin of the cells composing cluster 11. **L-O.** UMAPs of naive hPSCs, primed hPSCs, cells isolated from blastocyst-like structures and cells isolated from a CS7 staged human embryo. **L.** Coloration of stem cells based on their origin. **M.** Coloration of embryo cells based on previously proposed annotations[18]. **N.** Display of the expression levels of genes specific for each of the three blastocyst lineages (EPI - Epiblast, TE - Trophectoderm, and PrE- Primitive endoderm). **O.** Coloring of the cells previously identified as cluster 11 (see **H**). **P.** Quantification of the percentage of cells identified as abnormal based on the location in the UMAP in **O** (**top**) and on the cells annotations (**bottom**) for both naive hPSCs (**left**) and cells isolated from blastocyst-like structures (**right**). Similar results were obtained based on the location in the UMAP in **C-E**. **Q.** Gene expression heatmap for previously proposed markers of different lineages[19].

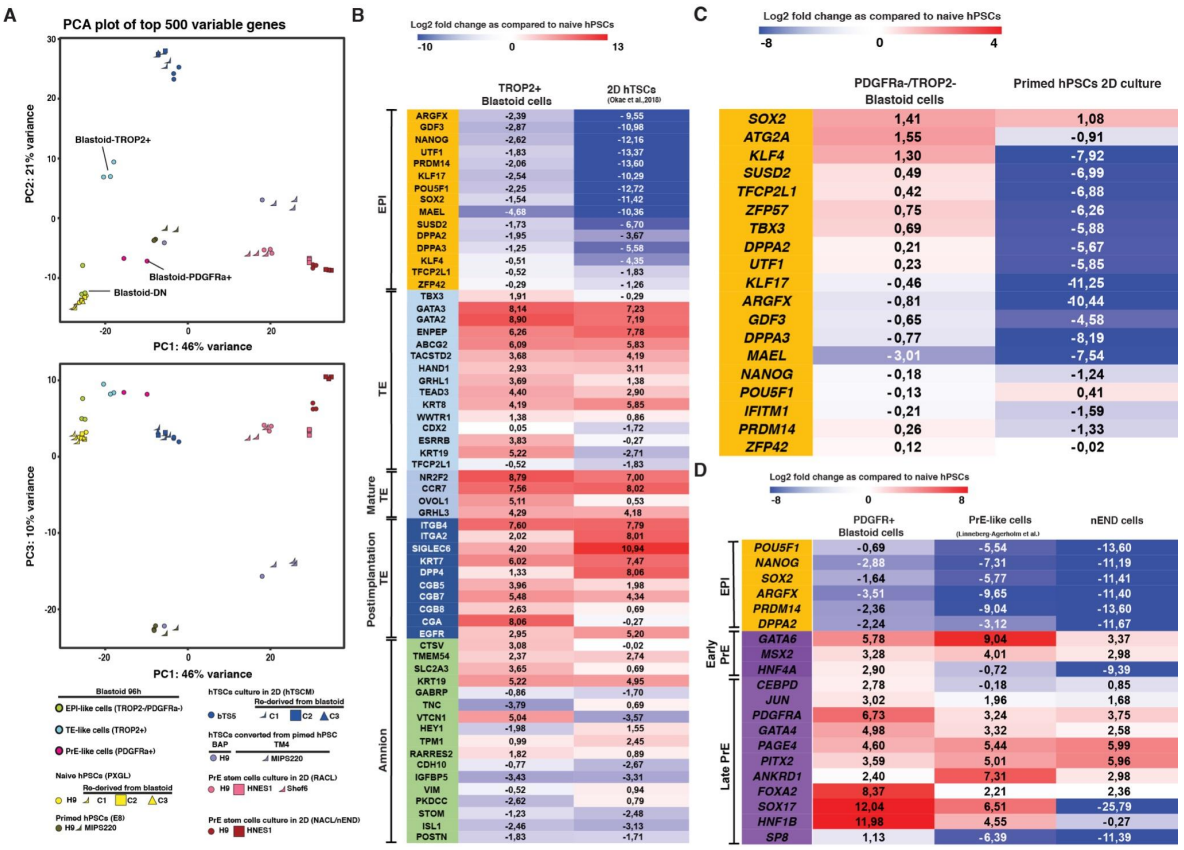
A
PCA plot of top 500 variable genes
Blastoid-TROP2+
Blastoid-PDGFRa+
Blastoid-DN
PC2: 21% variance
PC1: 46% variance
PC3: 10% variance
PC1: 46% variance
Blastoid 96h
EPI-like cells (TROP2-/PDGFRa-)
TE-like cells (TROP2+)
PrE-like cells (PDGFRa+)
Naive hPSCs (PXGL)
Re-derived from blastoid
H9 C1 C2 C3
Primed hPSCs (E8)
H9 MIPS220
hTSCs culture in 2D (hTSCM)
Re-derived from blastoid
bTS6 C1 C2 C3
hTSCs converted from pimed hPSC
BAP TM4
H9 MIPS220
PrE stom cells culture in 2D (RACL)
H9 HNES1 Shof6
PrE stom cells culture in 2D (NACL/nEND)
H9 HNES1
B
Log2 fold change as compared to naive hPSCs
-10 0 13
TROP2+ Blastoid cells
2D hTSCs (Okae et al.,2018)
EPI
TE
Mature TE
Postimplantation TE
Amnion
ARGFX -2,39 -9,55
GDF3 -2,87 -10,98
NANOG -2,62 -12,16
UTF1 -1,83 -13,37
PRDM14 -2,06 -13,60
KLF17 -2,54 -10,29
POU5F1 -2,25 -12,72
SOX2 -1,54 -11,42
MAEL -4,68 -10,36
SUSD2 -1,73 -6,70
DPPA2 -1,95 -3,67
DPPA3 -1,25 -5,53
KLF4 -0,51 -4,35
TFCP2L1 -0,52 -1,83
ZFP42 -0,29 -1,26
TBX3 1,91 -0,29
GATA3 8,14 7,23
GATA2 8,90 7,19
ENPEP 6,26 7,78
ABCG2 6,09 5,83
TACSTD2 3,68 4,19
HAND1 2,93 3,11
GRHL1 3,69 1,38
TEAD3 4,40 2,90
KRT8 4,19 5,85
WWTR1 1,38 0,86
CDX2 0,05 -1,72
ESRRB 3,83 -0,27
KRT19 5,22 -2,71
TFCP2L1 -0,52 -1,83
NR2F2 8,79 7,00
CCR7 7,56 8,02
OVOL1 5,11 0,53
GRHL3 4,29 4,18
ITGB4 7,60 7,79
ITGA2 2,02 8,01
SIGLEC6 4,20 10,94
KRT7 6,02 7,47
DPP4 1,33 8,06
CGB5 3,96 1,98
CGB7 5,48 4,34
CGB8 2,63 0,69
CGA 8,06 -0,27
EGFR 2,95 5,20
CTSV 3,08 -0,02
TMEM54 2,37 2,74
SLC2A3 3,65 0,69
KRT19 5,22 4,95
GABRP -0,86 -1,70
TNC -3,79 0,69
VTCN1 5,04 -3,57
HEY1 -1,98 1,55
TPM1 0,99 2,45
RARRES2 1,82 0,89
CDH10 -0,77 -2,67
IGFBP5 -3,43 -3,31
VIM -0,52 0,94
PKDCC -2,62 0,79
STOM -1,23 -2,48
ISL1 -2,46 -3,13
POSTN -1,83 -1,71
C
Log2 fold change as compared to naive hPSCs
-8 0 4
PDGFRa-/TROP2- Blastoid cells
Primed hPSCs 2D culture
SOX2 1,41 1,08
ATG2A 1,55 -0,91
KLF4 1,30 -7,92
SUSD2 0,49 -6,99
TFCP2L1 0,42 -6,88
ZFP57 0,75 -6,26
TBX3 0,69 -5,88
DPPA2 0,21 -5,67
UTF1 0,23 -5,85
KLF17 -0,46 -11,25
ARGFX -0,81 -10,44
GDF3 -0,65 -4,58
DPPA3 -0,77 -8,19
MAEL -3,01 -7,54
NANOG -0,18 -1,24
POU5F1 -0,13 0,41
IFITM1 -0,21 -1,59
PRDM14 0,26 -1,33
ZFP42 0,12 -0,02
D
Log2 fold change as compared to naive hPSCs
-8 0 8
PDGFR+ Blastoid cells
PrE-like cells (Linneberg-Agerholm et al.)
nEND cells
EPI
Early PrE
Late PrE
POU5F1 -0,69 -5,54 -13,60
NANOG -2,88 -7,31 -11,19
SOX2 -1,64 -5,77 -11,41
ARGFX -3,51 -9,65 -11,40
PRDM14 -2,36 -9,04 -13,60
DPPA2 -2,24 -3,12 -11,67
GATA6 5,78 9,04 3,37
MSX2 3,28 4,01 2,98
HNF4A 2,90 -0,72 -9,39
CEBPD 2,78 -0,18 0,85
JUN 3,02 1,96 1,68
PDGFRA 6,73 3,24 3,75
GATA4 4,98 3,32 2,58
PAGE4 4,60 5,44 5,99
PITX2 3,59 5,01 5,96
ANKRD1 2,40 7,31 2,98
FOXA2 8,37 2,21 2,36
SOX17 12,04 6,51 -25,79
HNF1B 11,98 4,55 -0,27
SP8 1,13 -6,39 -11,39

S3. Cells in human blastocyst-like structures are transcriptionally similar to pre-implantation lineages. A. Principal component analysis (PCA) plot with PC1 vs PC2 (**top**) or PC1 vs PC3 (**bottom**) computed with top 500 variable gene in the bulk transcriptome of individual lineages of blastocyst like structures (EPI, TE and PrE); stem cell lines: naive and primed hPSCs; hTSCs: blastocyst derived hTSCs (bTS5)[21], primed hPSC derived hTSCs (BAP[7] and TM4 protocols[22]; PrE like stem cell lines (RACL or nEND cells[25]); naive PSC and TSCs rederived from blastocyst-like structures (see methods). **B.** Heatmap of key blastocyst and post-implantation lineage markers differentially expressed between TE analogs ($TROP2^+$) of the blastocyst-like structures and hTSCs in their bulk transcriptome. **C.** Heatmap of key pluripotency related genes differentially expressed between EPI analogs ($PDGFR^-$/ $TROP2^-$) in the blastocyst-like structures and primed hPSCs. **D.** Heatmap of key pluripotency related genes or PrE markers differentially expressed between PrE analogs ($PDGFR\alpha^+$) in the blastocyst-like structures, naive PSC derived PrE-like cells and nEND cells.

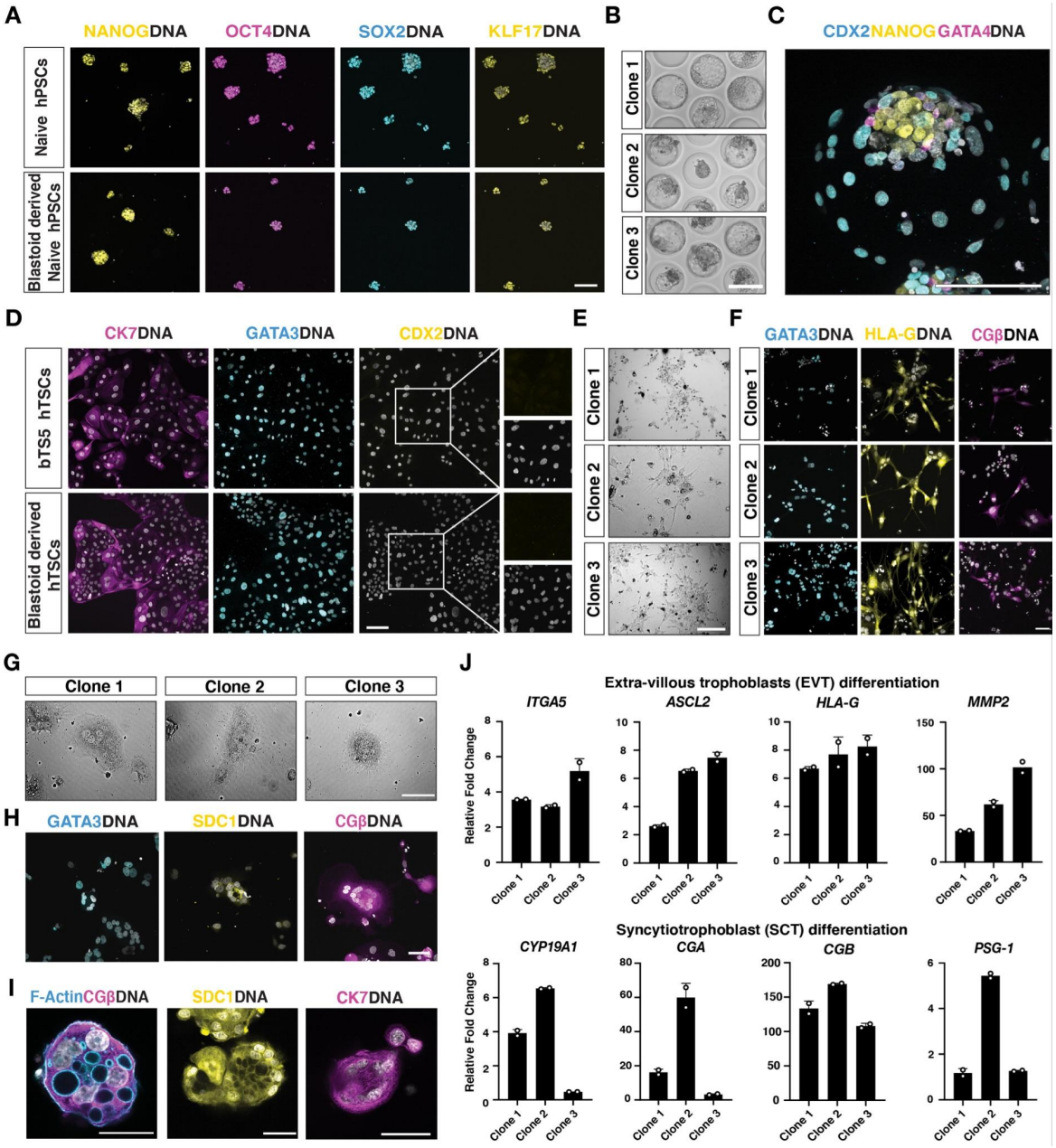
A
NANOGDNA
OCT4DNA
SOX2DNA
KLF17DNA
Naive hPSCs
Blastoid derived Naive hPSCs
B
Clone 1
Clone 2
Clone 3
C
CDX2NANOGGATA4DNA
D
CK7DNA
GATA3DNA
CDX2DNA
bTS5 hTSCs
Blastoid derived hTSCs
E
Clone 1
Clone 2
Clone 3
F
GATA3DNA
HLA-GDNA
CGβDNA
Clone 1
Clone 2
Clone 3
G
Clone 1
Clone 2
Clone 3
H
GATA3DNA
SDC1DNA
CGβDNA
I
F-ActinCGβDNA
SDC1DNA
CK7DNA
J
Extra-villous trophoblasts (EVT) differentiation
ITGA5
ASCL2
HLA-G
MMP2
Relative Fold Change
Clone 1
Clone 2
Clone 3
Syncytiotrophoblast (SCT) differentiation
CYP19A1
CGA
CGB
PSG-1

S4. Human blastocyst-like structures are permissive for derivation of stem cell lines. A. Immunofluorescence staining for pluripotency factors NANOG (Yellow), OCT4 (Magenta), SOX2 (Cyan) and for naive pluripotency factor KLF17 (Yellow) in naive hPSC controls (**top**) and naive hPSCs derived from blastocyst-like structures (**bottom**). **B.** Phase contrast images of blastocyst-like structures on microwell array formed from three rederived naive hPSC lines. Scale bar: 200 μm. **C.** Immunofluorescence stainings for EPI marker (NANOG), TE marker (CDX2) and primitive endoderm marker (GATA4) in representative second-generation blastocyst-like structures. Scale bar: 100 μm. **D.** Immunofluorescence staining for GATA3 (Cyan), post-implantation trophoblast marker CK7 (Magenta) and CDX2 (Yellow) in bTS5 hTSC (**top**) and hTSCs derived from blastocyst-like structures (**bottom**). **E.** Phase contrast images of day 6 EVT differentiations from three hTSC lines derived from blastocyst-like structures. Scale bar: 150 μm**F.** Immunofluorescence stainings of trophoblast markers GATA3 (Cyan) and EVT marker HLA-G (Yellow) and CGβ (Magenta) of day 6 EVT analogs from three hTSC lines, derived from blastocyst-like structures. Scale bar: 100 μm. **G.** Phase contrast images of day 3 SCT analogs differentiated from three hTSC lines derived from blastocyst-like structures Scale bar: 150 μm. **H.** Immunofluorescence stainings for trophoblast markers GATA3 (Cyan) and SCT marker SDC1 (Yellow) and CGβ (Magenta) of day 3 SCT analogs formed from hTSC line derived from blastocyst-like structure (Clone 1). Scale bar: 100 μm**I.** Immunofluorescence stainings for CGβ (Magenta) counterstained with Phalloidin (Cyan) and Hoechst marking Actin and DNA respectively (**left**), SDC (Yellow), CK7 (Magenta) (**right**) counterstained with Hoechst marking DNA of day 6 trophoblast organoids formed from hTSC lines derived from blastocyst-like structures (Clone 1). **J.** Relative expression levels, as measured by RT-PCR, of day 6 EVT (**top**) and day 3 SCT analogs (**bottom**) with respective undifferentiated hTSCs lines derived from blastocyst-like structures. Expression levels were normalized to expression of *GAPDH*. Error bars indicate S.D. from two technical duplicates.

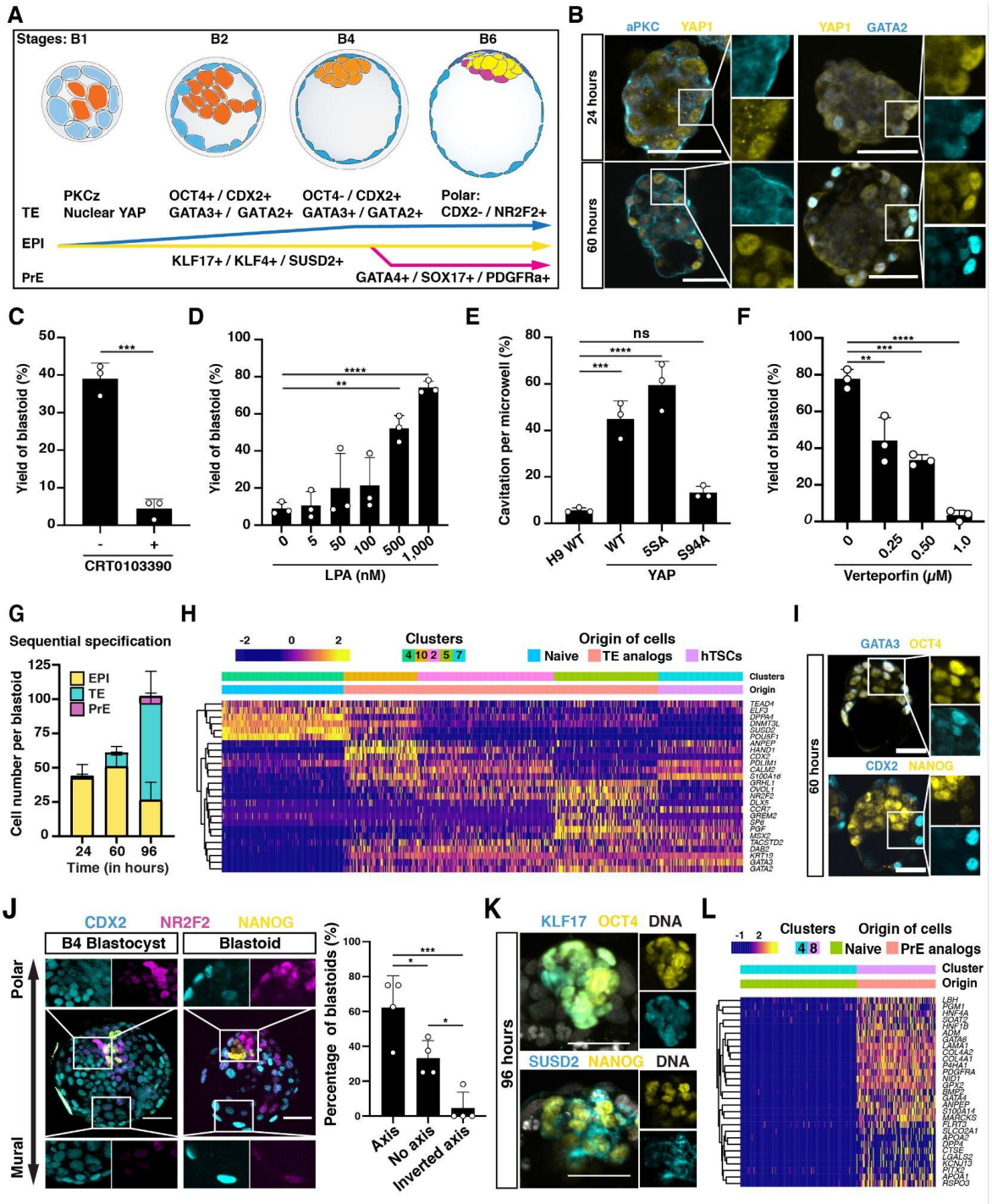
A
Stages: B1
B2
B4
B6
PKCz
Nuclear YAP
TE
OCT4+ / CDX2+
GATA3+ / GATA2+
OCT4- / CDX2+
GATA3+ / GATA2+
Polar:
CDX2- / NR2F2+
EPI
KLF17+ / KLF4+ / SUSD2+
PrE
GATA4+ / SOX17+ / PDGFRa+
B
aPKC
YAP1
YAP1
GATA2
24 hours
60 hours
C
Yield of blastoid (%)
CRT0103390
D
Yield of blastoid (%)
LPA (nM)
E
Cavitation per microwell (%)
ns
H9 WT
WT
5SA
S94A
YAP
F
Yield of blastoid (%)
Verteporfin (μM)
G
Sequential specification
Cell number per blastoid
EPI
TE
PrE
Time (in hours)
H
Clusters
Origin of cells
Naive
TE analogs
hTSCs
Clusters
Origin
I
GATA3
OCT4
CDX2
NANOG
60 hours
J
CDX2
NR2F2
NANOG
B4 Blastocyst
Blastoid
Polar
Mural
Percentage of blastoids (%)
Axis
No axis
Inverted axis
K
KLF17
OCT4
DNA
SUSD2
NANOG
DNA
96 hours
L
Clusters
Origin of cells
Naive
PrE analogs
Cluster
Origin

Figure 3: The three lineages form according to the sequence and time of blastocyst development. A. Schematic depicting the sequential development of human blastocysts. **B.** Immunofluorescence stainings for aPKC (Cyan) and YAP1 (Yellow) (**left**) and YAP1 (Yellow) with GATA3 (Cyan) (**right**) in aggregates of naive hPSCs cultured in PALLY medium. Counterstain with Hoechst marking DNA. Scale bar: 50 μm. **C**. Quantification of the yield of blastoids upon the culture in PALLY medium or PALLY medium complemented with an aPKC inhibitor (2 μM CRT0103390). n=3 independent microwell arrays, Error bar: S.D, Statistical analysis: Two tailed unpaired t-test. *** is P=0.0002. **D.** Dose dependent effect of LPA on the yield of blastoids. n=3 independent microwell arrays, Error bar: S.D, Statistical analysis: one-way Anova and Dunnett's multiple comparisons test, ** is P=0.0016; **** is P<0.0001. **E.** Measurement of the effect of the overexpression of different variants of YAP1 on cavitation events in early blastoids. n=3 experiments, Error bar: S.D, Statistical analysis: one-way Anova and Tukey's multiple comparisons test, ns is not significant, *** is P=0.0004; **** is P<0.0001. **F.** Measurement of the effect of Verteporfin (suppressor of the YAP1–TEAD complex) on the yield of blastoids. n=3 independent microwell arrays. **G.** Quantification of total cell numbers per lineage in developing blastoids at three time points of development (24, 60, 96h). **H.** Heatmap of the average count values in the expression of TE genes upon formation of the blastoid TE analogs. **I.** Immunofluorescence stainings for OCT4 (Yellow) and GATA3 (Cyan)(**top**) and NANOG (Yellow) and CDX2 (Cyan)(**bottom**) in aggregates of naive hPSCs cultured in PALLY medium for 60 hours. Scale bar: 50 μm. **J.** Immunofluorescence stainings for CDX2 (Cyan) NR2F2 (Magenta) and NANOG (Yellow) in representative B4-stage human blastocyst (**left**) and a blastoid (**middle**). Quantification of the proportion of blastoids with a preferentially polar NR2F2 expression pattern (axis) as compared to a preferentially mural NR2F2 expression pattern (inverted axis) (**right**). n=4 independent experiments with 4 to 12 blastoids in each experiment. Error bar: S.D. Statistical analysis: one-way Anova and Tukey's multiple comparisons test, * is P<0.05; *** is P<0.001. Scale bar: 50 μm. Error bar: S.D. **K.** Immunofluorescence staining of KLF17 (Cyan) and OCT4 (Yellow) (**top**) and SUSD2 (Cyan) and NANOG (Yellow) in EPI compartment of 96h blastoids. Counterstain with Hoechst marking DNA. Scale bar: 50 μm. **L.** Heatmap of the average count values in the expression of PrE genes upon formation of the blastoid PrE analogs.

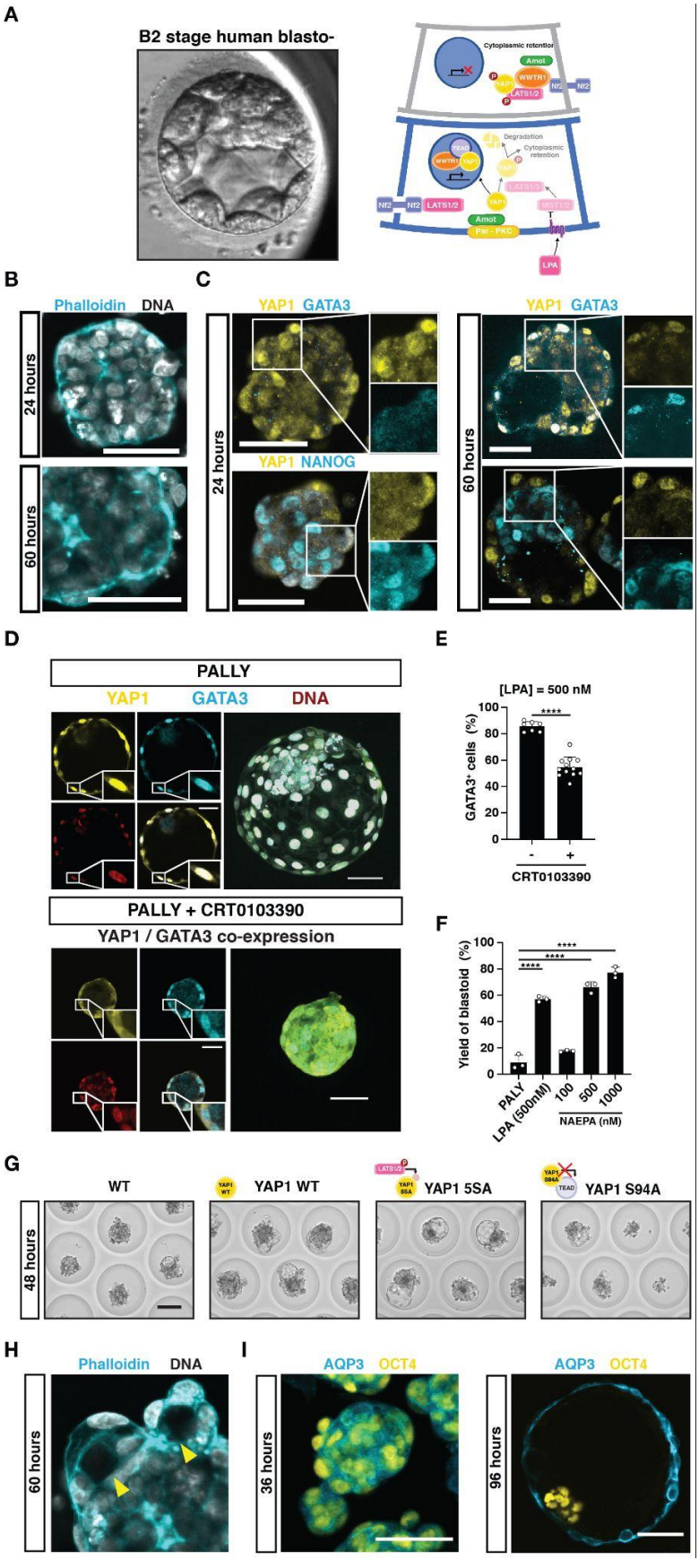
A
B2 stage human blasto-
Cytoplasmic retention
Amot
WWTR1
YAP1
LATS1/2
Nf2
Degradation
TEAD
Par - PKC
LPA
B
Phalloidin DNA
24 hours
60 hours
C
YAP1 GATA3
YAP1 NANOG
24 hours
60 hours
D
PALLY
YAP1 GATA3 DNA
PALLY + CRT0103390
YAP1 / GATA3 co-expression
E
[LPA] = 500 nM
GATA3+ cells (%)
CRT0103390
F
Yield of blastoid (%)
PALY
LPA (500nM)
NAEPA (nM)
G
WT
YAP1 WT
YAP1 5SA
YAP1 S94A
48 hours
H
Phalloidin DNA
60 hours
I
AQP3 OCT4
36 hours
96 hours

Figure S5: The development of the human trophectoderm analog depends on aPKC and Hippo elements. A. A frame from time-lapse microscopy of B2 stage human blastocyst (**left**). Schematic showing the differential Hippo activity in inner and outer cells of developing blastocyst and the molecular regulators of the Hippo signalling pathway (**right**). **B.** Phalloidin fluorescence (Cyan) stainings for F-actin in naive hPSCs aggregates cultured in PALLY medium for 24 hours (**top**) and 60 hours (**bottom**). Counterstain with Hoechst marking DNA. Scale bar: 50µm. **C.** Immunofluorescence stainings for YAP1 (Yellow) and GATA3 (Cyan) (**top**) and YAP1 (Yellow) and NANOG (Cyan) (**bottom**) in naive hPSCs aggregates cultured in PALLY medium for 24 hours (**left**) and 60 hours (**right**). Counterstain with Hoechst marking DNA. Scale bar: 50 µm. **D.** Immunofluorescence staining for YAP1 (Yellow) and GATA3 (Cyan) in blastoids cultured without (**top**) or with an aPKC inhibitor (2 µM CRT0103390, **bottom**). Counterstain with Hoechst marking DNA (Red). Insets: Individual and merge channels of YAP1 and GATA3 for a single optical section as well as maximum intensity projection of all the optical sections. Scale bar: 50 µm. **E.** Quantification of the percentage of $GATA3^{+}$ cells in structures cultured in PALLY medium or in PALLY medium complemented with a aPKC inhibitor (2 µM CRT0103390). n=7 blastoids for the group cultured in PALLY medium and n=12 aggregates for the group cultured in PALLY medium complemented with CRT0103390. Representative results from three independent experiments. Error bar: S.D, Statistical analysis: Two-tailed unpaired t-test. **** is $P<0.0001$ **F.** Quantification of the dose dependent effect of the LPA receptor agonist NAEPA on the yield of blastoids. The PALY medium (thus without LPA) was complemented with NAEPA. n=3 independent microwell arrays, Error bar: S.D, Statistical analysis: one-way Anova and Tukey's multiple comparisons test. **** is $P<0.0001$. **G.** Phase contrast images of representative naive hPSC aggregates cultured in PALLY medium complemented with Doxycycline (100 ng/ml) for 72 hours and overexpressing different variants of YAP1. The naive hPSCs aggregates were cultured with an adjusted PALLY medium characterized by a reduced LPA concentration (5 nM). Scale bar: 100 µm. **H.** Phalloidin fluorescence staining of F-actin (Cyan) in naive hPSCs aggregates cultured in PALLY medium for 60 hours. Counterstain with Hoechst marking DNA. Yellow arrows: Formation of cavities. Scale bar: 50 µm. **I.** Immunofluorescence stainings for Aquaporin3 (AQP3, Cyan) and OCT4 (Yellow) in naive hPSCs aggregates cultured in PALLY medium for 36 (**left**) or 96 hours (**right**, blastoid stage). Scale bar: 50 µm.

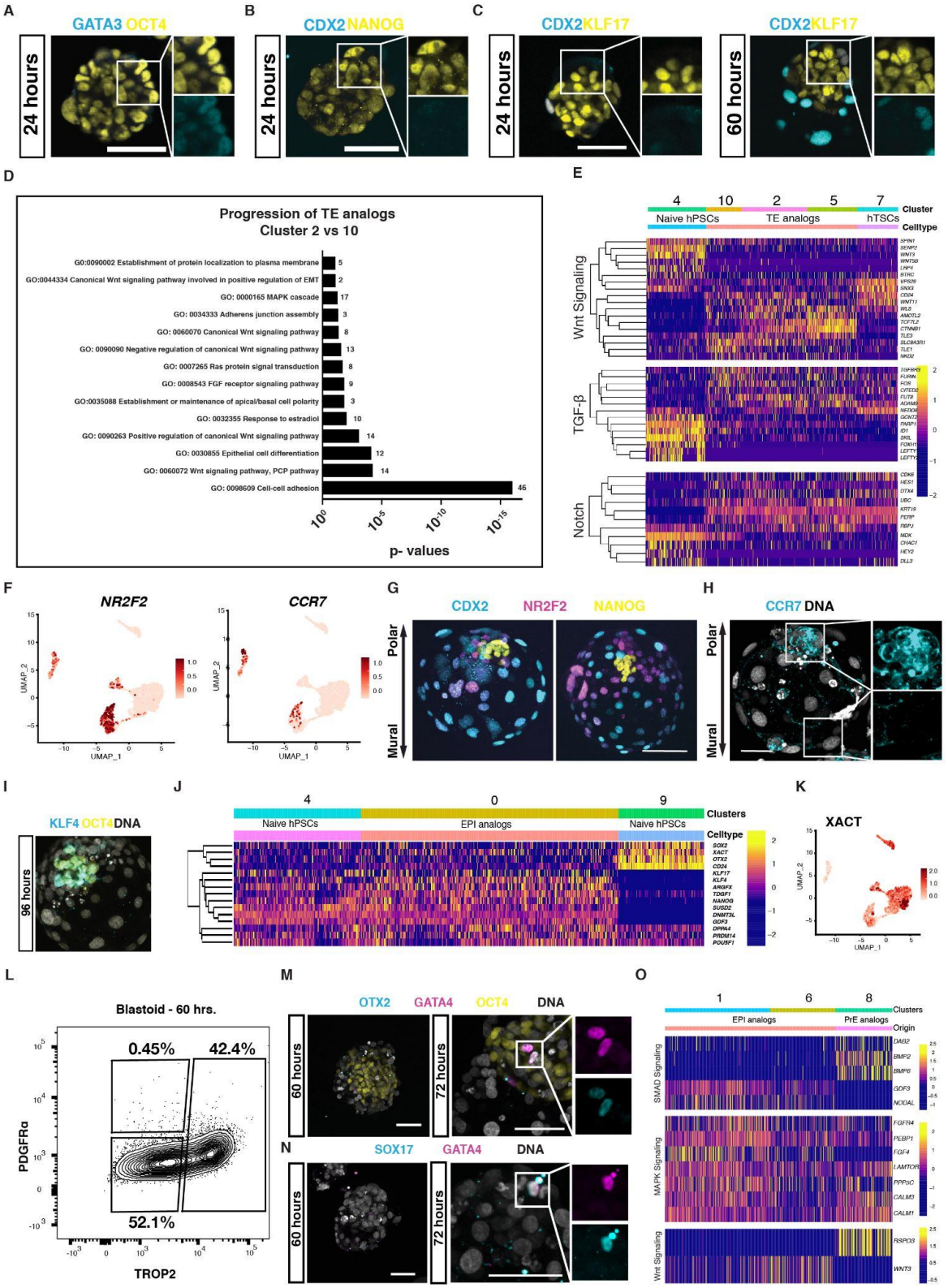
A
GATA3 OCT4
24 hours
B
CDX2 NANOG
24 hours
C
CDX2 KLF17
24 hours
CDX2 KLF17
60 hours
D
Progression of TE analogs
Cluster 2 vs 10
G0:0090002 Establishment of protein localization to plasma membrane
GO:0044334 Canonical Wnt signaling pathway involved in positive regulation of EMT
GO: 0000165 MAPK cascade
GO: 0034333 Adherens junction assembly
GO: 0060070 Canonical Wnt signaling pathway
GO: 0090090 Negative regulation of canonical Wnt signaling pathway
GO: 0007265 Ras protein signal transduction
GO: 0008543 FGF receptor signaling pathway
GO:0035088 Establishment or maintenance of apical/basal cell polarity
GO: 0032355 Response to estradiol
GO: 0090263 Positive regulation of canonical Wnt signaling pathway
GO: 0030855 Epithelial cell differentiation
GO: 0060072 Wnt signaling pathway, PCP pathway
GO: 0098609 Cell-cell adhesion
5
2
17
3
8
13
8
9
3
10
14
12
14
46
p- values
E
4 10 2 5 7
Cluster
Naive hPSCs
TE analogs
hTSCs
Celltype
Wnt Signaling
TGF-β
Notch
F
NR2F2
CCR7
UMAP_1
UMAP_2
G
CDX2 NR2F2 NANOG
Polar
Mural
H
CCR7 DNA
Polar
Mural
I
KLF4 OCT4 DNA
96 hours
J
4 0 9
Clusters
Naive hPSCs
EPI analogs
Naive hPSCs
Celltype
K
XACT
UMAP_1
UMAP_2
L
Blastoid - 60 hrs.
0.45%
42.4%
52.1%
PDGFRα
TROP2
M
OTX2 GATA4 OCT4 DNA
60 hours
72 hours
N
SOX17 GATA4 DNA
60 hours
72 hours
O
1 6 8
Clusters
EPI analogs
PrE analogs
Origin
SMAD Signaling
MAPK Signaling
Wnt Signaling

Figure S6. Blastoids recapitulate the sequential specification of lineages occurring during blastocyst development. A, B. Immunofluorescence stainings for GATA3 (Cyan)) and OCT4 (Yellow) or CDX2 (Cyan) and NANOG (Yellow) in naive hPSCs aggregates cultured in PALLY medium for 24 hours. Scale bar: 50 µm. **C.** Immunofluorescence stainings for CDX2 (Cyan) and KLF17 (Yellow) in naive hPSCs aggregates cultured in PALLY medium for 24 (**left**) and 60 hours (**right**). Scale bar: 50 µm. **D.** Gene ontology terms associated with the genes, differentially regulated in the late TE analog of blastoids (cluster 10) as compared to the early TE (cluster 2). **E.** Heatmap of average count values of Wnt, TGF-β and Notch signaling-associated genes in cells from cluster 4 (naive hPSCs), 10, 2 and 5 (TE analogs) and 7 (TSC). **F.** UMAPs of single cells isolated from blastoids and displaying the expression levels of polar trophectoderm specific genes: NR2F2 and CCR7. **G.** Immunofluorescence staining for CDX2 (Cyan), NR2F2 (Magenta) and NANOG (Yellow) in blastoids. Scale bar: 100 µm. **H.** Immunofluorescence stainings for CCR7 (Cyan) in a blastoid. Counterstain with Hoechst marking DNA. Scale bar: 50 µm. **I.** Immunofluorescence staining for KLF4 (Cyan) and OCT4 (Yellow) in blastoids. Counterstain with Hoechst marking DNA. Scale bar: 50 µm. **J.** Heatmap of average count values of top differentially regulated genes in cells from cluster 4 (naive hPSCs), 0 (EPI analogs) and 9 (primed hPSCs). **K.** UMAPs of single cells isolated from blastoids and displaying the expression levels of X chromosome activation-related gene-*XACT.* **L** Flow cytometry analysis plot of cells isolated from blastocyst-like structures and stained for lineage-specific surface markers PDGFRa (PrE) and TROP2 (TE)**. M, N.** Immunofluorescence stainings for OTX2 (Cyan), GATA4 (Magenta) and OCT4 (Yellow) (**M)** and SOX17 (Cyan) and GATA4 (Magenta) (**N**) in naive hPSCs aggregates cultured in PALLY medium for 60 hours. Counterstain with Hoechst marking DNA. Scale bar: 50 µm. **O.** Heatmap of average count values of SMAD, MAPK and Wnt signaling-associated genes in cells from cluster 1, 6 (EPI analogs) and 8 (PrE analogs).

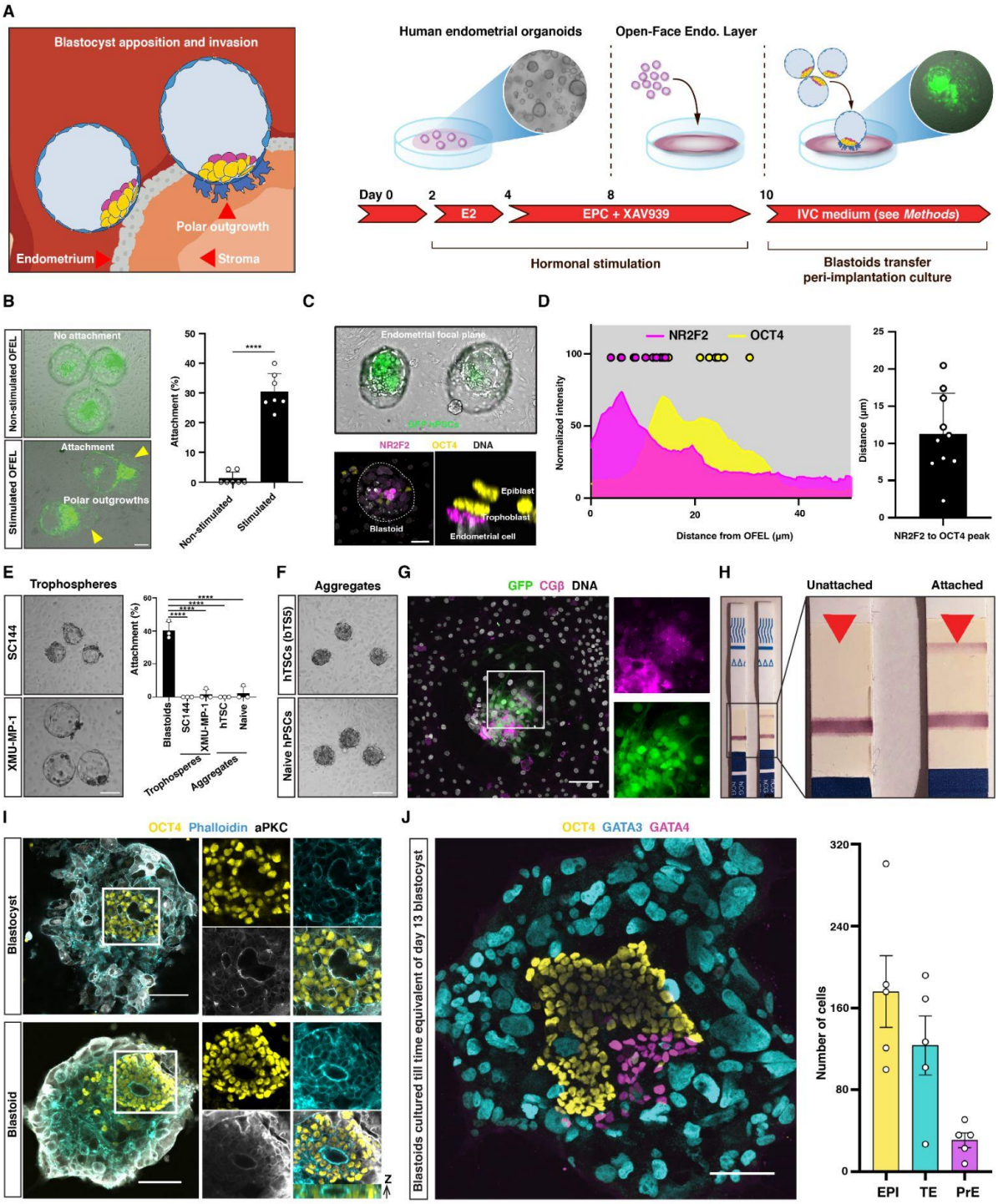
A
Blastocyst apposition and invasion
Polar outgrowth
Endometrium
Stroma
Human endometrial organoids
Open-Face Endo. Layer
Day 0
2
4
8
10
E2
EPC + XAV939
IVC medium (see Methods)
Hormonal stimulation
Blastoids transfer
peri-implantation culture
B
Non-stimulated OFEL
Stimulated OFEL
No attachment
Attachment
Polar outgrowths
Attachment (%)
****
Non-stimulated
Stimulated
C
Endometrial focal plane
GFP-hPSCs
NR2F2
OCT4
DNA
Blastoid
Epiblast
Trophoblast
Endometrial cell
D
NR2F2
OCT4
Normalized intensity
Distance from OFEL (μm)
Distance (μm)
NR2F2 to OCT4 peak
E
Trophospheres
SC144
XMU-MP-1
Attachment (%)
Blastoids
SC144
XMU-MP-1
hTSC
Naive
Trophospheres
Aggregates
F
Aggregates
hTSCs (bTS5)
Naive hPSCs
G
GFP CGβ DNA
H
Unattached
Attached
I
OCT4 Phalloidin aPKC
Blastocyst
Blastoid
Z
J
OCT4 GATA3 GATA4
Blastoids cultured till time equivalent of day 13 blastocyst
Number of cells
EPI
TE
PrE

Figure 4: Human blastoids recapitulate aspects of implantation. A. Schematic showing the time window of human implantation hereby modeled (**left**). Two-step protocol of formation of an Open Face Endometrial Layer (OFEL) and of blastoid deposition as an *in vitro* implantation assay (**right**). OFELs are primed for receptivity by complementing the culture medium with EPC/XAV939. E2: Beta-estradiol. EPC: **E**2, **P**rogesteron, **c**AMP. **B.** Representative phase contrast images of blastoids (GFP^+) 24 hours after deposition onto non-stimulated (**top left**) or stimulated (**bottom left**) OFELs**.** Scale bar: 100 µm. Quantification of the attachment efficiency of human blastoids to unstimulated and stimulated OFELs (**right**). n=7 independent experiments from 3 different donors. Horizontal bars indicate mean percentage. Error bar: S.D. Statistical analysis; Unpaired two-tailed *t*-test, **** is $P < 0.0001$. **C.** Representative images of human blastoids shortly after attachment to an OFEL (12 ± 4 hours). Dotted line outlines the inner cluster of blastoids that were formed using GFP^+ naive hPSCs (**top**, also see **Sup video 3**). Immunofluorescence stainings for NR2F2 (Magenta) and OCT4 (Yellow) in blastoids shortly after attachment to an OFEL (**bottom left**). X-Z plane of the previous image (**bottom right**). Scale bar: 50 µm. **D.** Fluorescence intensity profile of immunofluorescence stainings for NR2F2 and OCT4 in blastoids shortly after attachment to an OFEL (**left**). Profiles were measured perpendicular to the plane of attachment. Quantification of the distance between the first peak of fluorescence intensity profiles of NR2F2 and OCT4 **(right)**. n=10 attached blastoids. Error Bar: S.D. **E.** Representative phase contrast images of trophospheres formed by adding 3 µM SC144 (**top left**) or 2 µM XMU-MP-1 (**bottom left**) during blastoid formation and then deposited onto stimulated OFELs. Scale bar: 100 µm. Quantification of the attachment efficiency of trophospheres and aggregates deposited onto stimulated OFELs (**right**). n=3 independent experiments. Horizontal bars indicate mean percentage. Error bar: S.D. Statistical analysis: one-way Anova and Dunnett's multiple comparisons test, **** is $P < 0.0001$. **F.** Representative phase contrast images of aggregates of hTSCs or naive hPSCs, deposited onto stimulated OFELs. Scale bar: 100 µm. **G.** Immunofluorescence staining for the syncytiotrophoblast-associated marker CGβ (Magenta) in GFP^+ blastoids attached onto stimulated OFELs (48 hours after deposition). Counterstain with Hoechst marking DNA. Scale bar: 50 µm. **H.** Detection of human chorionic gonadotropin (CGβ) secretion into the culture medium of unstimulated OFELs with unattached blastoids (**left**) and stimulated OFELs with attached blastoids (**right**) by using pregnancy test strips (48 hours, also see ELISA assay in **Sup. Fig. 9B**). **I.** Immunofluorescence stainings for OCT4 (Yellow) and aPKC (Grey) in human blastocysts (**top**) or blastoids (**bottom**) grown in postimplantation culture condition for 4 days. Counterstain with Phalloidin marking F-actin (Cyan). Scale bar: 100µm. **J.** Immunofluorescence stainings for OCT4 (Yellow), GATA3 (Cyan) and GATA4 (Magenta) in blastoids grown in postimplantation culture condition for 6 days corresponding to time equivalent of day 13 of cultured human blastocyst (**left**). Scale bar: 100µm. Quantification of the number of cells positive for OCT4, GATA3, and GATA4 (**right**), n=5 blastoids. Error bar: S.D.

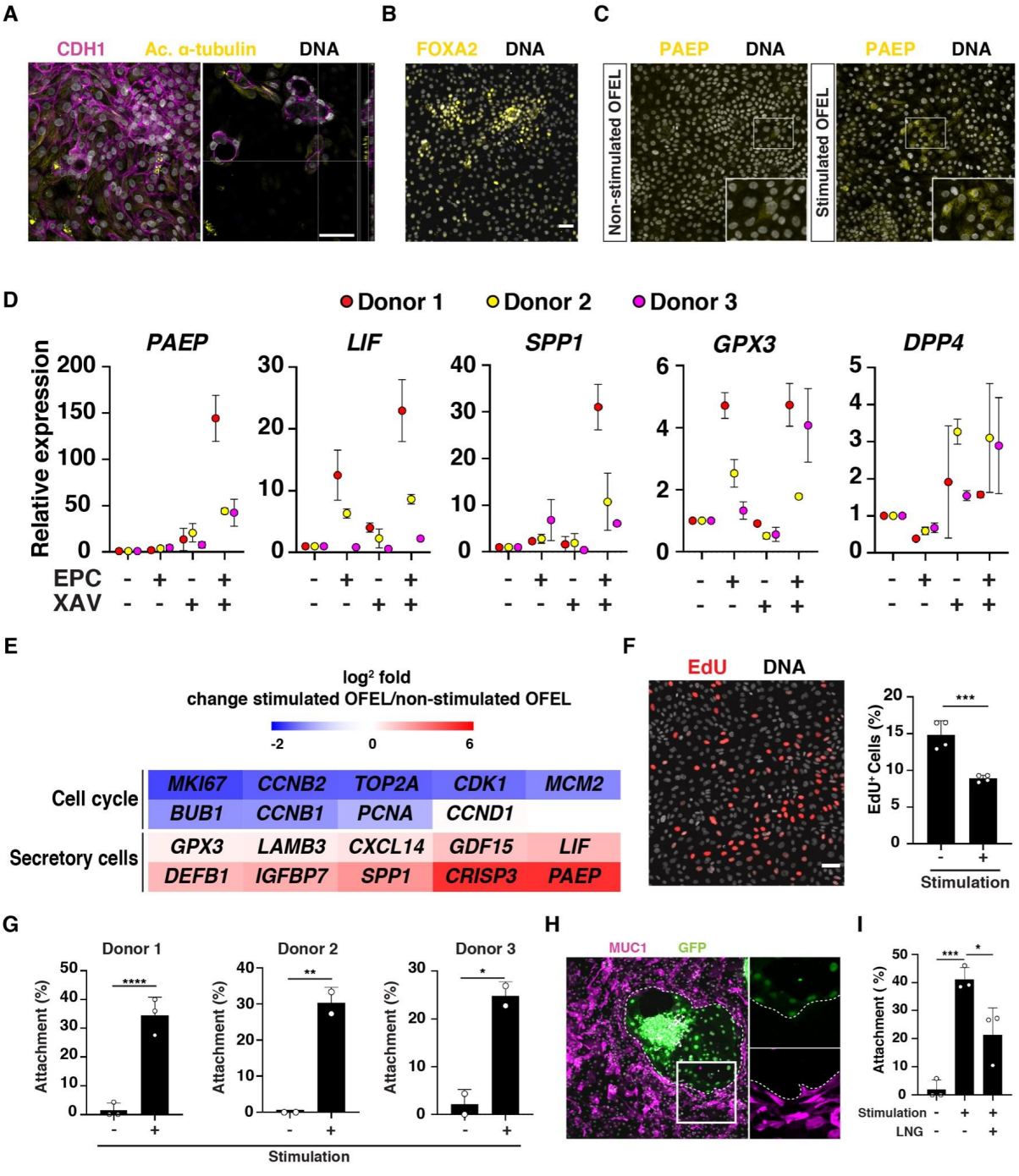
A
CDH1
Ac. α-tubulin
DNA
B
FOXA2
DNA
C
PAEP
DNA
Non-stimulated OFEL
PAEP
DNA
Stimulated OFEL
D
Donor 1
Donor 2
Donor 3
PAEP
LIF
SPP1
GPX3
DPP4
Relative expression
EPC
XAV
E
log² fold
change stimulated OFEL/non-stimulated OFEL
-2
0
6
Cell cycle
MKI67
CCNB2
TOP2A
CDK1
MCM2
BUB1
CCNB1
PCNA
CCND1
Secretory cells
GPX3
LAMB3
CXCL14
GDF15
LIF
DEFB1
IGFBP7
SPP1
CRISP3
PAEP
F
EdU
DNA
EdU⁺Cells (%)
Stimulation
G
Donor 1
Donor 2
Donor 3
Attachment (%)
Stimulation
H
MUC1
GFP
I
Attachment (%)
Stimulation
LNG

Figure S7: Human blastoids recapitulate aspects of endometrium implantation.
A. Immunofluorescence stainings for CDH1(Magenta) and ciliated cell marker acetylated α-tubulin (Yellow) in OFELs (**left**). Y-Z plane shows the apical location of the cilia (**right**). Scale bar: 50 µm. **B.** Immunofluorescence staining for FOXA2 (Yellow) marking the endometrial glandular cells in OFELs. Scale bar: 50 µm. **C.** qRT-PCR measurement of the expression levels of window-of-implantation markers in OFELs cultured with different media. Ctrl: Control medium, E: Estradiol, P: Progesterone, C: cAMP, X: XAV-939. Expression levels were normalized relative to the housekeeping gene GAPDH and the control condition. Error bar: S.D. The colors depict the data from 3 different donors. **D.** Immunofluorescence staining for PAEP (Yellow) in non-stimulated (**left**) and stimulated (**right**) OFELs. **E.** Heatmaps showing log2 fold change of cell cycle and secretory epithelial marker genes between stimulated and non-stimulated OFELs in bulk transcriptome. **F.** Immunofluorescence staining for incorporated EdU (Red) reflective of cell proliferation in a stimulated OFEL (**left**). Scale bar: 50 µm. Quantification of the number of EdU^+ cells in unstimulated and stimulated OFELs (**right**). n=4 independent experiments. Horizontal bars indicate mean percentage. Error bar: S.D. Statistical analysis: Unpaired two-tailed *t*-test, *** is $P = 0.0009$. **G.** Quantification of blastoid attachment onto OFELs formed using endometrial organoids from 3 different donors. Horizontal bars indicate mean percentage. Error bar: S.D. Statistical analysis: one-way Anova and Tukey's multiple comparisons test for donor 1 and unpaired two-tailed *t*-test for donor 2 and 3, * is $P < 0.05$, ** is $P < 0.01$, **** is $P < 0.0001$. **H.** Immunofluorescence stainings for MUC1 (Magenta), a glycoprotein that highly expresses at the luminal epithelial surface of endometrium in the receptive phase[52], in attached GFP+ blastoid (24 hours after deposition onto an OFEL). Dashed lines indicate the area that trophoblast cells repelled endometrial cells **I.** Quantification of blastoid attachment onto unstimulated, stimulated OFELs, and OFELs additionally exposed to the contraceptive Levonorgestrel (LNG, 10 µM). n=3 independent experiments. Horizontal bars indicate mean percentage. Error bar: S.D. Statistical analysis: one-way Anova and Tukey's multiple comparisons test, * is $P < 0.05$, *** is $P = 0.0006$.

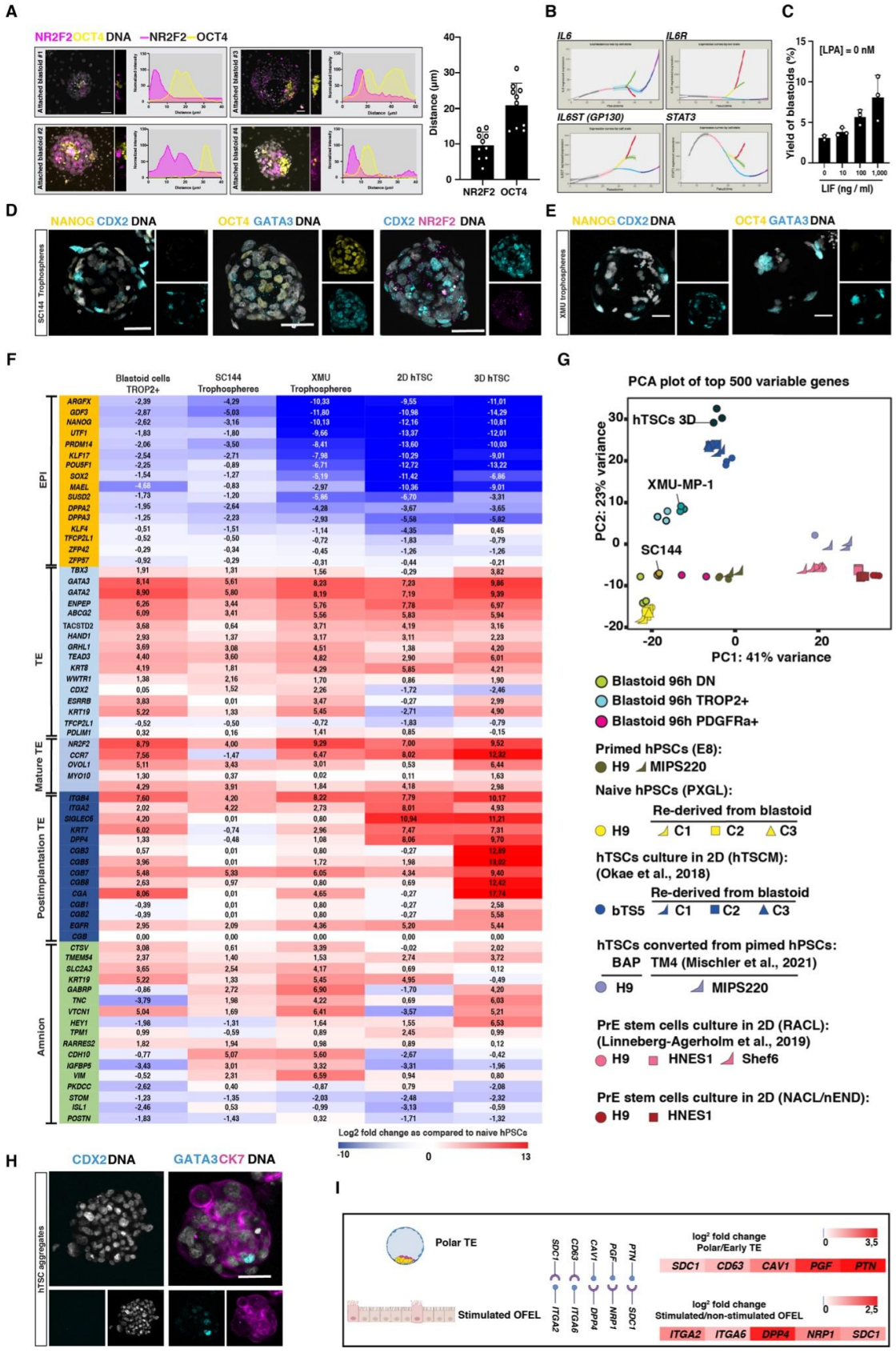
A
NR2F2 OCT4 DNA
NR2F2
OCT4
Attached blastoid #1
Attached blastoid #2
Attached blastoid #3
Attached blastoid #4
Distance (µm)
NR2F2
OCT4
B
IL6
IL6R
IL6ST (GP130)
STAT3
C
[LPA] = 0 nM
Yield of blastoids (%)
LIF (ng / ml)
D
NANOG CDX2 DNA
OCT4 GATA3 DNA
CDX2 NR2F2 DNA
SC144 Trophospheres
E
NANOG CDX2 DNA
OCT4 GATA3 DNA
XMU trophospheres
F
Blastoid cells TROP2+
SC144 Trophospheres
XMU Trophospheres
2D hTSC
3D hTSC
EPI
TE
Mature TE
Postimplantation TE
Amnion
Log2 fold change as compared to naive hPSCs
G
PCA plot of top 500 variable genes
hTSCs 3D
XMU-MP-1
SC144
PC2: 23% variance
PC1: 41% variance
Blastoid 96h DN
Blastoid 96h TROP2+
Blastoid 96h PDGFRa+
Primed hPSCs (E8):
H9
MIPS220
Naive hPSCs (PXGL):
Re-derived from blastoid
H9
C1
C2
C3
hTSCs culture in 2D (hTSCM):
(Okae et al., 2018)
Re-derived from blastoid
bTS5
C1
C2
C3
hTSCs converted from pimed hPSCs:
BAP
TM4 (Mischler et al., 2021)
H9
MIPS220
PrE stem cells culture in 2D (RACL):
(Linneberg-Agerholm et al., 2019)
H9
HNES1
Shef6
PrE stem cells culture in 2D (NACL/nEND):
H9
HNES1
H
CDX2 DNA
GATA3 CK7 DNA
hTSC aggregates
I
Polar TE
Stimulated OFEL
SDC1
CD63
CAV1
PGF
PTN
ITGA2
ITGA6
DPP4
NRP1
SDC1
log2 fold change
Polar/Early TE
SDC1
CD63
CAV1
PGF
PTN
log2 fold change
Stimulated/non-stimulated OFEL
ITGA2
ITGA6
DPP4
NRP1
SDC1

Figure S8: Trophectoderm state is crucial for interaction with endometrium during implantation. A. Fluorescence intensity profiles of immunofluorescence stainings for NR2F2 (Magenta) and OCT4 (Yellow) in blastoids attached onto OFEL. Profiles were measured perpendicular to the plane of attachment (**right**). Line width, 10 µm. **B.** Pseudotime analysis of human pre-implantation development showing the expression of *IL6*, *IL6R*, *GP130* and *STAT3*. Gene expression analysis is performed by using the public data analysis tool (https://bird2cluster.univ-nantes.fr/demo/PseudoTimeUI/). **C.** Quantification of the dose dependent effect of LIF on the yield of blastoids. **D.** Immunofluorescence staining for NANOG (Yellow) and CDX2 (Cyan) (**left**) OCT4 (Yellow) and GATA3 (Cyan) (**middle**) and CDX2 (Cyan) and NR2F2 (Magenta) (**right**) in a representative trophosphere formed from a blastoid exposed to SC144. Scale bar: 50 µm. **E.** Immunofluorescence staining for NANOG (Yellow) and CDX2 (Cyan) (**left**) OCT4 (Yellow) and GATA3 (Cyan) (**right**) in a representative trophosphere formed from a blastoid exposed to XMU-MT-1. Scale bar: 50 µm. Heatmap showing differential expression of selected lineage specific genes in bulk transcriptome of the trophectoderm of blastoids (TROP2 positive cells), trophospheres (SC144 or XMU) and TSCs (2D or 3D) compared to naive hPSCs. **G.** PCA computed using bulk transcriptome of blastoid cells, hPSCs (naive, primed or blastoid rederived naive cell lines), TSCs (bTS5, blastocyst rederived lines or human stem cell derived TSC like cells) and pluripotent stem cell derived primitive endoderm like cells (RACL or NACL cells). **H.** Immunofluorescence stainings for CDX2 (Cyan) (**left**) and CK7 (Magenta) and GATA3 (Cyan) (**right**) in aggregates formed from bTS5 hTSCs. Counterstain with Hoechst marking DNA. Scale bar: 50 µm. **I.** List of selected putative ligand-receptor pairs involved in cross-talk between polar trophectoderm and endometrial epithelium during implantation. The list was generated by in silico ligand receptor analysis of genes enriched in polar trophectoderm and stimulated OFEL, using Cellinker[53].

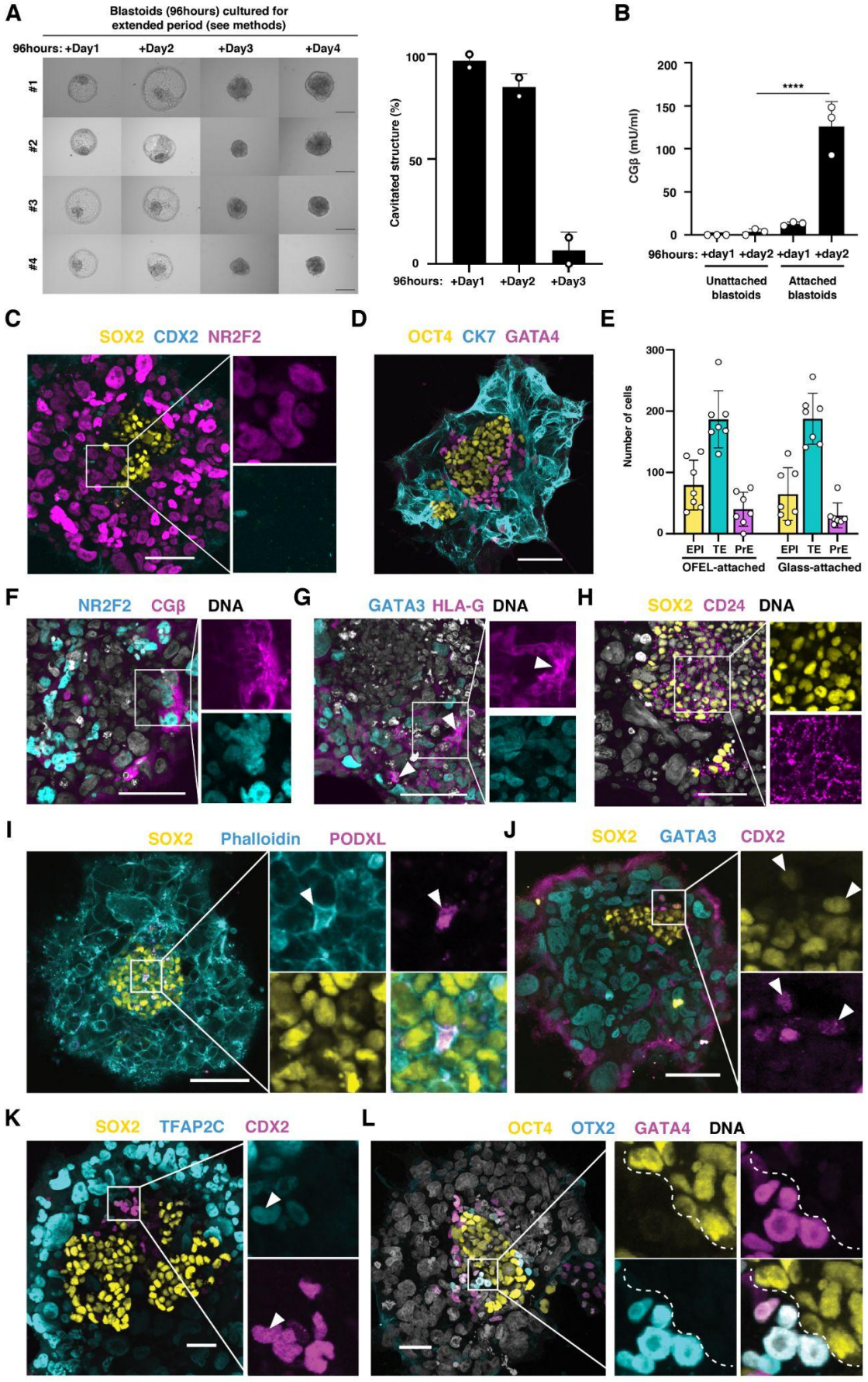
A
Blastoids (96hours) cultured for extended period (see methods)
96hours: +Day1
+Day2
+Day3
+Day4
#1
#2
#3
#4
Cavitated structure (%)
100
50
0
96hours: +Day1 +Day2 +Day3
B
CGβ (mU/ml)
200
150
100
50
0
****
96hours: +day1 +day2 +day1 +day2
Unattached blastoids
Attached blastoids
C
SOX2 CDX2 NR2F2
D
OCT4 CK7 GATA4
E
Number of cells
300
200
100
0
EPI TE PrE EPI TE PrE
OFEL-attached
Glass-attached
F
NR2F2 CGβ DNA
G
GATA3 HLA-G DNA
H
SOX2 CD24 DNA
I
SOX2 Phalloidin PODXL
J
SOX2 GATA3 CDX2
K
SOX2 TFAP2C CDX2
L
OCT4 OTX2 GATA4 DNA

Figure S9: Human blastoids recapitulate aspects of peri-implantation progression until day 13. A. Bright-field images of human blastoids (96hours) cultured for 4 additional days on a low attachment plate in post implantation culture condition. Each row shows a time series of an individual blastoid for 4 days. Note that, blastoids stably retain cavities at least for 2 days upon transferring to IVC media which has different osmolarity compared to the N2B27 media with PALLY. (See the methods for the composition of post implantation culture media.) Scale bar: 200 μm. Quantification of percentage of blastoids retaining cavities on each day of postimplantation stage culture. Error bar: S.D. **B.** ELISA measurements of the concentration of the protein CGβ secreted into the culture medium of unstimulated OFELs with unattached blastoids and stimulated OFELs with attached blastoids (24 and 48 hours). n=3 independent experiments. Horizontal bars indicate mean percentage. Error bar: S.D. Statistical analysis: one-way Anova and Tukey's multiple comparisons test, **** is $P < 0.0001$. **C.** Immunofluorescence stainings for CDX2 (Cyan), NR2F2 (Magenta) and SOX2 (Yellow) in blastoids grown in postimplantation culture condition for 4 days. Scale bar: 100μm. **D.** Immunofluorescence stainings for OCT4 (Yellow), CK7 (Cyan) and GATA4 (Magenta) in blastoids grown in postimplantation culture condition for 4 days. Scale bar: 100μm. **E.** Quantification of number of cells belonging to EPI, TE or PrE lineages in the blastoids cultured in postimplantation culture condition for four days on glass or OFEL. Error ber: S.D. **F-G.** Immunofluorescence stainings for CGβ (Magenta) and NR2F2 (Cyan) (**F**) or HLA-G (Magenta) and GATA3 (Cyan) (**G**), in blastoids grown in postimplantation culture condition for 4 days (**F**) or 6 days (**G**). Counterstain with Hoechst marking DNA. Arrowhead points HLA-G positive EVT like cells. Scale bar: 100μm. **H.** Immunofluorescence stainings for CD24 (Magenta) and SOX2 (Yellow) in blastoids grown in postimplantation culture condition for 4 days. Counterstain with Hoechst marking DNA. Scale bar: 100μm. **I.** Immunofluorescence stainings for PODXL (Magenta) and SOX2 (Yellow) in blastoids grown in postimplantation culture condition for 4 days. Counterstain with Phalloidin marking F-actin (Cyan). Arrowhead points pro-amniotic-like cavity. Scale bar: 100μm. **J-L.** Immunofluorescence stainings for SOX2 (Yellow), GATA3 (Cyan) and CDX2 (Magenta) (**J**), SOX2 (Yellow), CDX2 (Magenta) and TFAP2C (Cyan) (**K**), OCT4 (Yellow), GATA4 (Magenta) and OTX2 (Cyan) (**L**) in blastoids grown in postimplantation culture condition for 4 days. Counterstain with Hoechst marking DNA. Scale bar: 100μm.

METHODS

Culture of human naive pluripotent stem cells

Experiments were done using the following hPSC lines; hESC lines: H9, Shef6 and HNES1. hiPSC lines: cR-NCRM2 and niPSC 16.2.b. The H9 and H9-GFP lines reset to the naive state were provided by the laboratory of Yasuhiro Takashima. Other naive hESCs and hiPSCs were provided by the laboratory of Austin Smith. Naive hPSCs were cultured on gelatin-coated plates including a feeder layer of gamma-irradiated mouse embryonic fibroblasts (MEFs) in PXGL medium, as previously reported[54]. PXGL medium is prepared using N2B27 basal medium supplemented with PD0325901(1 μM, MedChemExpress, HY-10254), XAV-939 (1 μM, MedChemExpress, HY-15147), Gö 6983 (2 μM, MedChemExpress, HY-13689) and human leukaemia inhibitory factor (hLIF, 10 ng/ml, in-house made) as previously reported[54]. N2B27 basal medium contained DMEM/F12 (50%, in house made), Neurobasal medium (50%, in-house made), N2 supplement (Thermo Fisher Science, 17502048), B-27 supplement (Thermo Fisher Science, 17504044), GultaMAX supplement (Thermo Fisher Science, 35050-038), Non-essential amino acid, 2-Mercaptoethanol (100 μM, Thermo Fisher Science, 31350010), and Bovine Serum Albumin solution (0.45%, Sigma-Aldrich, A7979-50ML). Cells were routinely passaged as single cells every three to four days.

Culture of primed pluripotent ESCs

Primed H9 cells were cultured on Vitronectin XF (STEMCELL Technologies, 07180) coated plates (1.0 ug /cm2) using Essential 8 medium (in-house made).

Microwell arrays

Microwell arrays comprising microwells of 200 μm diameter were imprinted into 96-well plates as previously described[9,55].

Induction of blastoids and trophospheres

Naive hPSCs or primed hPSCs cultures were treated with Accutase (Biozym, B423201) at 37°C for 5 min, followed by gentle mechanical dissociation with a pipette. After centrifugation, the cell pellet was resuspended in PXGL medium, supplemented with Y-27632 (10 μM, MedChemExpress, HY-10583). To exclude MEF, the cell suspension was transferred onto gelatin coated plates and incubated at 37°C for 70 min. After MEF exclusion, the cell number was determined using a Countess™ automated cell counter (Thermo Fisher Scientific) and Trypan Blue staining to assess cell viability. The cells were then resuspended in N2B27 media containing 10 μM Y-27632 (aggregation medium) and 3.0 x 10^4 cells were seeded onto a microwell array included into a well of a 96-well plate. The cells were allowed to form aggregates inside the microwell for a period ranging from 0 to 24 hours depending on the cell lines and based on their propensity for aggregation. Subsequently, the aggregation medium was replaced with PALLY medium – N2B27 supplemented with PD0325901 (1 μM), A 83-01 (1 μM, MedChemExpress, HY-10432), hLIF (10 ng/ml), 1-Oleoyl lysophosphatidic acid sodium salt (LPA) (500nM, Tocris, 3854) and Y-27632 (10 μM). The PALLY medium was refreshed every 24 hours. After 48 hours, the PALLY medium was replaced with N2B27 medium containing 500 nM LPA and 10 μM Y-27632. At 96 hours, a blastoid is defined based on morphological similarity to B6 staged human blastocyst, as a structure composed of a monolayered cyst with an overall diameter

of 150-200 µm comprising one inner cell cluster. Blastoids reproducibly formed at high efficiency and we did not observe differences based on the number of passages after resetting in PXGL culture conditions. The effect of LPA, NAEPA (Sigma-Aldrich, N0912) and Verteporfin (Selleck Chemicals Llc, S1786) on the yield of blastoid formation was assessed by culturing naive hPSC aggregates in PALY medium complemented with molecules added every day from 0 to 96 hours. The Verteporfin treatment was executed without exposure to the light. The effect of the aPKC inhibitor CRT0103390 (Gift from the laboratory of Kathy Niakan) was assessed by culturing naive hPSC aggregates in PALLY medium complemented with 2 µM CRT0103390 every day from 0 to 96 hours. The formation of trophospheres was induced by culturing naive hPSC aggregates in PALLY medium complemented with 2 µM XMU-MP-1 (Med Chem Express, HY-100526) or 3 µM SC-144 (Axon, 2324) every day from 0 to 96 hours. The BSA concentration was titrated within the range of 0-0.3% for individual cell lines used for the formation of the blastoids and trophospheres.

Derivation of cell lines from human blastoids

Derivation experiments were performed with blastoids cultured for 96 hours as described in the previous section. Blastoids were individually transferred on gelatin coated 96-well plates with feeder layers of gamma-irradiated MEFs. Naive hPSCs were derived in PXGL medium[26]. hTSCs were derived in human trophoblast stem cell (hTSC) medium[21]. After 24 hours of culture on feeders, blastoids attached and, within one week, colonies were formed. Derivation was considered successful after three passages after blastoid transfer. For immunofluorescence assays, naive hPSCs were transferred onto Geltrex (0.5 µL/cm^2) coated coverslips, and hTSCs were transferred onto Fibronectin coated coverslips (5ug/ml, Sigma Aldrich, 08012).

Trophoblast organoid formation

Organoid formation was performed with blastoid derived hTSC lines. Organoids were cultured as previously described[56] with some modifications. Colonies of hTSCs were dissociated into single cells using 1xTrypsin at 37°C for 5 min. After centrifugation, 200.000 cells were resuspended in 150 ul Matrigel (Cornig, 356231). Droplets of 20ul per well were placed into a prewarmed 48-well cell culture plate and placed upside down into the incubator for 20 min. Organoids were cultured in 250ul TOM medium (Advanced DMEM-F12, N2 supplement, B27 supplement minus vitamin a, PenStrep, N-Acetyl-L-Cysteine (1.25mM), L-glutamine (2mM), A83-01 (500nM), CHIR99021 (1.5uM), recombinant human EGF (50ng/ml), 10% R-Spondin 1 conditioned medium, recombinant human FGF2 (100ng/ml), recombinant human HGF (50ng/ml), PGE2 (2.5.uM). Medium was refreshed every other day. For SCT formation organoids were maintained in TOM medium until day 7.

2D Trophoblast differentiations

The differentiation of blastoid derived hTSCs was performed as described previously[21] with some modifications. hTSC lines were adapted to Fibronectin coating (5ug/ml, Sigma Aldrich, 08012) for at least three passages prior to the experiments. For EVT and SCT differentiation, cells were dissociated with TrypLE for 5 min at 37°C and cells were seeded at a density of 55.000 cells/well onto 12-well plates. For SCT differentiation, the plates were precoated with 10ug/ml Fibronectin and cultured in SCT medium (DMEM/F12, supplemented with 0.1 mM 2-mercaptoethanol, 0.5% Penicillin-Streptomycin, 1% ITS-X supplement, 7.5 mM A83-01,

2.5 mM Y27632, 4% KnockOut Serum Replacement and 2 mM forskolin) for 3 days. For EVT differentiation, plates were precoated with Matrigel and cells were cultured in EVT medium (DMEM/F12, supplemented with 0.1 mM 2-mercaptoethanol, 0.5% Penicillin-Streptomycin, 1% ITS-X supplement, 2% Matrigel, 7.5 mM A83-01, 2.5 mM Y27632, 4% KnockOut Serum Replacement and 100 ng/ml NRG1,). After three days, the medium was changed to EVT medium with 0.5% Matrigel and without NRG1. Cells were cultured until day 6.

Human pre-implantation embryos culture

Human embryos were thawed following the manufacturer's instructions (Cook Medical: Sydney IVF Thawing kit for slow freezing and Vitrolife: RapidWarmCleave or RapidWarmBlast for vitrification). Human embryos frozen at 8-cell stage were loaded in a 12-well dish (Vitrolife: Embryoslide Ibidi) with non-sequential culture media (Vitrolife G2 plus) under mineral oil (Origio: Liquid Paraffin), at 37°C, in 5% O2/6% CO2.

Plasmid construction

The cDNA sequence of hYAP1, hYAP1 5SA, and hYAP1 5SA + S94A were amplified from the pQCXIH-Myc-YAP, pQCXIH-Myc-YAP-5SA, pQCXIH-Myc-YAP-S94A plasmids respectively. These YAP plasmids were gifts from Kunliang Guan (Addgene plasmid # 33091, #33093 and #33094)[31]. The individual cDNA sequences were cloned into pDONR211, followed by cloning into PB-TAC-ERP2 using Gateway (invitrogen) cloning strategy. PB-TAC-ERP2 was a gift from Knut Woltjen (Addgene plasmid #80478)[57]. Complete sequences of resulting plasmids are available upon request.

Cell transfection in human naive PSCs

pCAG-PBase (5 µg) and PB-TAC-YAP1-ERP (5 µg) were transfected by NEPA21 electroporation (Nepa Gene Co. Ltd) into 5 x 10^4 cells in single-cell suspension. Electroporated naive hPSCs were plated on Geltrex (0.5 µL/cm^2, Thermo Fisher Science, A1413302)-coated 6-well plates with PXGL medium containing Y-27632 (10 µM) . Puromycin (0.5 ug/ml, Sigma-aldrich, P7255) was added to PXGL medium from day 1 to day 3-4 to select transformed cells. pCAG-PBase was a gift from Knut Woltjen.

YAP overexpression in naive hPSC aggregates

The naive hPSC aggregates were formed from naive H9 cell lines integrated with the doxycycline inducible cassette as described in the section above. The aggregates were cultured in PALLY medium with reduced LPA concentration (5 nM) from 0 hours to 48 hours along with 100 ng/ml Doxycycline. Higher LPA concentrations masked the effects of the genetic overexpression of the YAP1 variants. The number of cavitated aggregates were counted at 72 hours.

Single cell RNA-seq library preparation and sequencing

To avoid over-representation of TE cells, blastoids were collected, dissociated and the cell suspension was stained using antibodies against TROP2 and PDGFRa that mark trophoblasts and primitive endoderm, respectively. For the 96 hours time point, blastoids were selectively picked up from the microwell arrays before the dissociation, according to the morphological criteria described above. Cells were FACS-sorted into 384 well-plates containing the lysis buffer for Smart-seq2 and immediately frozen. The antibody staining was

exploited in order to harvest specific numbers of TROP2+, PDGFRa+ and double-negative cells. The abuted FACS gates covered the whole spectrum and no blastoid cells were excluded. The H9 naive cells cultured on MEF were stained using an antibody against SUSD2, then FACS-sorted. Dead cells were excluded by DAPI staining. Smart-seq2 libraries were generated as described previously with minor optimization[58]. Maxima H Minus reverse transcriptase (3U/reaction, Thermo Fisher Science, EP0751) was used for the cDNA synthesis. The prepared libraries were sequenced on the S1 or SP flow cell using an Illumina Novaseq instrument in 50 bp paired end mode.

Single cell RNA-seq data analysis

Smart-Seq transcriptome sequencing experiments were analysed using genome sequence and gene annotation from Ensembl GRCh38 release 103 as reference.

For gene expression quantification RNA-seq reads were first trimmed using trim-galore v0.6.6 and thereafter aligned to the human genome (Ensembl GRCh38 release 103) using hisat2 v2.2.1. Uniquely mapping reads in genes were quantified using htseq-count v0.13.5 with parameter -s no. TPM estimates were obtained using RSEM v1.3.3 with parameter --single-cell-prior.

Further analysis was performed in R v4.0.3 with Seurat v4.0.1. Based on initial evaluation of per-cell quality control metrics and outlier identification using the median absolute deviation algorithm, cells with <= 2000 detected genes or >= 12.5% mitochondrial gene percentage were filtered out. Only genes detected in at least 5 cells were retained. Count-data were log-normalized, top 3000 highly variable were selected, and standardization of per gene expression values across cells was performed using NormalizeData, FindVariableFeatures and ScaleData data functions in Seurat. Principal component analysis (PCA) based on the standardized highly variable features was used for linear dimension reduction, a shared nearest neighbor (SNN) graph was constructed on the dimensionally reduced data, and the graph was partitioned using a SNN modularity optimization based clustering algorithm at a range of resolutions using RunPCA, FindNeighbors and FindClusters from Seurat with default settings. Cluster marker genes were identified with the Wilcox likelihood-ratio test using the FindAllMarkers function. Uniform Manifold Approximation and Projection (UMAP) was used for visualization.

For integration of Smart-Seq experiments from multiple sources we followed the previously described procedure[19]. Published data from GSE109555, E-MTAB-3929 were downloaded and data from Carnegie stage 7 embryo was kindly provided by the authors[18]. All the data was preprocessed to obtain per gene read counts using the same protocol as described for blastoid cells, in the case of GSE109555 including adaptations to accommodate UMI and CB information following the authors instructions (https://github.com/WRui/Post_Implantation). For GSE109555 we used 1000 cells randomly subsampled from the 3184 high quality single cells described in the original publication. Similar to [19] we excluded cells belonging to hemogenic endothelial progenitors and erythroblasts. After evaluation of per-cell quality control metrics, and as in [19], cells with > 2000 detected genes and < 12.5% mitochondrial gene percentage were retained. Genes detected in at least five cells in any dataset were retained. Log-normalization was performed using computeSumFactors in scran package v1.18.7, per-batch scaling normalization using multiBatchNorm in batchelor v1.6.3. Datasets were aligned using the fastMNN approach via SeuratWrappers v0.3.0 using the log-normalized batch-adjusted expression values. MNN low-dimensional coordinates were then used for clustering and visualization by Uniform Manifold Approximation and Projection (UMAP).

Culture of human trophoblast stem cells and aggregate formation

Experiments were performed using the human blastocyst-derived hTSC line bTS5 provided by the laboratory of Takahiro Arima. Cells were cultured on Laminin 511 (5 µg/ml, BioLamina, LN511) coated plates in hTSC medium as previously described[21]. Aggregates of hTSCs were formed as follows. Colonies were dissociated into single cells using Accutase at 37°C for 5 min. The cells were resuspended into hTSC medium containing 10 µM Y-27632, and 3.0 x 10^4 cells were seeded onto a microwell array imprinted into a well of a 96-well plate. The same medium[21] was refreshed daily. After 72 hours, the aggregates were used for both characterisation and implantation experiments.

Endometrial organoid culture

Cryopreserved human endometrial organoids were provided by the Hossein Baharvand laboratory (Royan Institute) within the framework of collaboration agreements. Human endometrial organoids were established from healthy human donors following the protocol described previously[37,59] with some modifications. Briefly, organoids were cultured in human endometrial expansion medium composed of 10% Rspo1 conditioned medium (in-house made) and 10% Noggin-Fc-conditioned medium[60] (in-house made), supplemented with 1× N2 supplement , 1× B27 supplement , 1X Insulin-Transferrin-Selenium (in-house), Glutamax (1 µM), N-acetylcysteine (1.25 mM, Sigma-Aldrich, A7250), nicotinamide (2.5 mM, Sigma-Aldrich, 72340), EGF (50 ng/ml, Peprotech, 100-47), bFGF (2 ng/ml, Peprotech, 100-18B), HGF (10 ng/ml, Peprotech, 315-23), FGF10 (10 ng/ml, Peprotech, 100-26), A83-01 (500 nM) and SB202190 (10 µM, Tocris, 1264). Y-27632 (10 µM) was used in the first 2 days after passaging to prevent apoptosis. The medium was changed every 2 days and the organoids were passaged with TrypLE followed by mechanical dissociation every 7-9 days.

Hormonal stimulation of endometrial organoids and OFELs culture

Endometrial organoids were passaged as described in the previous section. The dissociated cells were resuspended in Matrigel supplemented with Y-27632 (10 µM), cell suspension was deposited in 48-well plates and were cultured in endometrial expansion medium for 2 days. The organoids were stimulated first with E2 (10 nM, Sigma-Aldrich, E2758) for 2 days, followed by the mixture of E2 (10 nM), P4 (1 µM, Sigma-Aldrich, P8783), and cAMP (250 µM, Biolog, B 007) with or without XAV939 (10 µM) (EPC or EPCX respectively) for 4 days. For OFELs culture, organoids were recovered from the matrigel droplets with ice-cold DMEM/F12 and mechanical pipetting. The organoids were dissociated using TrypLE and mechanically triturated to generate single cells and seeded at the density of 3 to 3,5 x 10^4 cells per wells into a 96-well glass bottom plate (Cellvis, P96-1.5H-N) and cultured for 2 days with stimulation. For contraceptive treatment, levonorgestrel (LNG) (10 µM, Sigma-Aldrich, PHR1850) was added to the medium for two days after hormonal stimulation and continued until the end of experiment.

***In vitro* implantation assay**

Confluent OFELs were prepared for the implantation assay at least 2 hours prior to the deposition of blastoids, trophospheres, naive- or hTSC aggregates by washing the OFEL two times with DMEM/F12 and adding IVC medium[47]. Structures were then transferred onto the OFELs using a mouth pipette under an inverted microscope. After 24 hours, the medium was removed, the well was washed with PBS, fixed using 4% formaldehyde for 30 minutes

at room temperature and subsequently processed for immunofluorescence staining. The percentage of attached structures was reported as the percentage of total transferred structures.

In vitro culture of human blastoids in post implantation conditions

Human blastoids were selected using a mouth pipette, washed with CMRL1066 medium and transferred into suspension culture plates or 96-well plates coated with Matrigel containing pre-equilibrated media adapted from monkey blastocyst culture[46] with minor modifications as followed. For the first day, the culture medium was CMRL1066 supplemented with 10% (v/v) FBS, 1 mM l-glutamine (Gibco), 1× N2 supplement, 1× B27 supplement, 1 mM sodium pyruvate (Sigma) and 10 μM Y27632. After 24h, half of the medium was replaced with new medium including 5% Matrigel. After 48h, 50% of medium was replaced with new medium supplemented with 20% (v/v) FBS and 5% Matrigel. After 72 h, half of the medium was replaced with new medium supplemented with 30% (v/v) KSR and 5% Matrigel. Then, half of the medium was replaced every day and blastoids were cultured for up to 6 days. Cultures were fixed for staining after 4 and 6 days of in vitro culture with 4% PFA as mentioned above.

Human pre-implantation embryos

The use of human embryos donated to research as surplus of IVF treatment was allowed by the French embryo research oversight committee: Agence de la Biomédecine, under approval number RE13-010 and RE18-010. All human pre-implantation embryos used in this study were obtained from and cultured at the Assisted Reproductive Technology unit of the University Hospital of Nantes, France, which are authorized to collect embryos for research under approval number AG110126AMP of the Agence de la Biomédecine. Embryos used were initially created in the context of an assisted reproductive cycle with a clear reproductive aim and then voluntarily donated for research once the patients have fulfilled their reproductive needs or tested positive for the presence of monogenic diseases. Informed written consent was obtained from both parents of all couples that donated spare embryos following IVF treatment. Before giving consent, people donating embryos were provided with all of the necessary information about the research project and opportunity to receive counselling. No financial inducements are offered for donation. Molecular analysis of the embryos was performed in compliance with the embryo research oversight committee and The International Society for Stem Cell Research (ISSCR) guidelines[61].

RNA extraction, cDNA synthesis and qRT-PCR

RNA was extracted using the RNeasy mini kit (Qiagen, 74106) and cDNA synthesis was performed using the Superscript III (Invitrogen, 18080093) enzyme. qPCR reactions were performed using GoTaq® qPCR Master Mix (Promega, A6001) on CFX384 Touch Real-Time PCR Detection System (Bio-rad). Quantification was performed using Microsoft Office Excel by applying the comparative Cycle threshold (Ct) method. Relative expression levels were normalized to GAPDH. The primers used for the qPCR analysis are listed in Supplementary Table 2**.**

ELISA assay for CGβ detection

Media from wells containing unattached and attached blastoids was collected and centrifuged to remove debris and stored at −80 °C until use. The supernatant was subject to

CGβ ELISA (Abcam, ab178633), according to the manufacturer's instructions, alongside CGβ standards.

Ligand-receptor Analysis

Cellinker platform was used to predict putative receptor-ligand interactions between polar TE and endometrial epithelial cells. Genes within the NR2F2 module for late TE[23], enriched genes in polar TE, gene module for endometrial epithelial cells that marked the entrance into phase 4 of menstrual cycle[40] along with upregulated genes in stimulated OFELs were used as the query to search ligands and receptors in the database.

Immunohistochemistry

The samples were fixed with 4% formaldehyde for 30 minutes at room temperature. Post fixation, formaldehyde solution was removed and the samples were washed at least three times with PBS. The samples were then permeabilized and blocked using 0.3% triton-x 100 and 10% normal donkey serum in PBS for at least 60 minutes. The samples were then incubated overnight at 4°C with primary antibodies diluted in fresh blocking/permeabilization solution. The samples were washed with PBS containing 0.1% triton-x100 (PBST) for at least three times for 10 minutes each. The washing buffer was then replaced with Alexafluor tagged secondary antibodies (Abcam or Thermofisher scientific) along with a nuclear dye Hoechst-33342 (1:500 or 1:300 for 2D or 3D samples respectively, Life Technologies, H3570) diluted in PBST for 30 minutes in dark at room temperature. The samples were then washed with PBST three times for 10 minutes each. For human blastocysts, the samples were fixed at the B4 or B6 stage according to the grading system proposed by Gardner and Schoolcraft[62]or at B3 or B4 + 72 hours in vitro culture. Embryos were fixed with 4% paraformaldehyde for 10min at room temperature and washed in PBS/BSA. Embryos were permeabilized and blocked in PBS containing 0.2% Triton-x100 and 10% FBS at room temperature for 60 min. Samples were incubated with primary antibodies overnight at 4°C. Incubation with secondary antibodies was performed for 2 hours at room temperature along with Hoechst counterstaining. The samples were mounted for imaging in PBS in the wells of glass bottom micro slides (Ibidi, 81507). The details of antibodies and their dilutions are provided in the supplementary table 1. EdU staining was done using Click-iT EdU Alexa Fluor 647 Imaging Kit (Thermo Scientific, C10640) following the manufacturer's instructions.

Microscopy and image analysis

The phase contrast images were acquired using Thermo Fisher scientific EVOS cell imaging system and inverted wide field microscope Axio VertA1. The number of blastoids or cavitated structures were counted manually for each well. After 96 hours, a blastoid is defined based on the morphological parameters as described in previous sections. The fluorescent images and time-lapse images were acquired using Olympus IX83 microscope with Yokogawa W1 spinning disk (Software: CellSense ; camera: Hamamatsu Orca Flash 4.0) or Nikon Eclipse Ti E inverted microscope, equipped with a Yokogawa W1 spinning disc (Software: Visiview ; camera:Andor Ixon Ultra 888 EMCCD)**.** The confocal images were analyzed and display images were exported using FIJI or Bitplane Imaris softwares. For cell counting, Bitplane Imaris software was used. Cell count parameters were set for size and fluorescence strength of voxels and then overall cell count data was obtained for each image using Imaris's spot function. Note that large cavities in blastoids increase the depth of the imaging field causing poor signal from deeply located cells. Therefore, our counting data in figure 1H and 3G could

be underrepresented values, particularly in the case of trophectoderm cells. The quantification of the percentage of blastoids forming the NR2F2 axis was done manually. To do so, blastoids stained to detect NR2F2 expression were imaged using a confocal-spinning disk microscope. The images were projected using a 3D-project function in FIJI. The blastoid was classified to have an axis when NR2F2 expression was restricted to its polar half with no expression or lower level of expression in the mural half. The inverted pattern of NR2F2 expression was classified as an invert axis. The blastoids with NR2F2 expression on their both polar and mural halves were classified to have no axis. Confocal immunofluorescence images of human blastocysts were acquired with a Nikon confocal microscope and a 20× Mim or 25x Silicon objective. Optical sections of 1 µm-thick were collected. The images were processed using Fiji (http://fiji.sc) and Volocity 6.3 visualization softwares. Volocity software was used to detect and count nuclei.

Data availability

Single cell RNA-sequencing and bulk RNA sequencing data for human blastoids used in this study were deposited at the GEO repository under the accession number GSE177689.

Ethical approvals

The use of human embryos donated to research as surplus of IVF treatment was allowed by the French embryo research oversight committee: Agence de la Biomédecine, under approval number RE13-010 and RE18-010. All human pre-implantation embryos used in this study were obtained from and cultured at the Assisted Reproductive Technology unit of the University Hospital of Nantes, France, which are authorized to collect embryos for research under approval number AG110126AMP of the Agence de la Biomédecine. Human endometrium samples were obtained from patients who signed an informed consent form and protocols approved by the Ethics Committee of Royan Institute (IR.ACECR.ROYAN.REC. 1397.93) and ethical approval from the Ethics Committee of the Shahid Beheshti University of Medical Sciences (IR.SBMU.MSP.REC. 1396.25). The Wicell line H9 was used under the agreement 20-WO-341 for a research program entitled 'Modeling early human development: Establishing a stem cell based 3D in vitro model of human blastocyst (blastoids)'. Blastoid generation was approved by the Commission for Science Ethics of the Austrian Academy of Sciences. All experiments complied with all relevant guidelines and regulations, including the 2021 ISSCR guidelines.

Acknowledgment

This project has received funding from the European Research Council (ERC) under the European Union’s Horizon 2020 research and innovation programme (ERC-Co grant agreement No.101002317 'BLASTOID: a discovery platform for early human embryogenesis'). HHK is supported by the Austrian Science Fund (FWF), Lise Meitner Programme M3131-B. This project has also received funding from the ANR “BOOSTIVF”. LD thanks the iPSCDTC and MicroPICell core facilities. We thank Yasuhiro Takashima for sharing the H9 and H9-GFP cell lines, and Austin Smith, Peter Andrews, and Ge Guo for sharing the HNES1, Shef6, niPSC 16.2b and cR-NCRM2 cell lines. We thank Hossein Baharvand for sharing the endometrial organoids, Knut Woltjen for sharing the PB-TAC-ERP2 and pCAG-PBase plasmids, and Kunliang Guan for sharing pQCXIH-Myc-YAP, pQCXIH-Myc-YAP-5SA, pQCXIH-Myc-YAP-S94A plasmids. We thank Aleksand Bykov and Luisa Cochella for technical assistance for SMARTSeq2 library

preparation. We thank the NGS, Biooptic and Stem Cell facility at IMBA for critical assistance.

Conflict of interest

HK, AJ, HHK, and NR are inventors on the patent application EP21151455.9 describing these results.

1. Rivron, N. *et al.* Debate ethics of embryo models from stem cells. *Nature* **564**, 183–185 (2018).
2. Stephenson, R. O., Rossant, J. & Tam, P. P. L. Intercellular interactions, position, and polarity in establishing blastocyst cell lineages and embryonic axes. *Cold Spring Harb. Perspect. Biol.* **4**, (2012).
3. Bredenkamp, N. *et al.* Wnt Inhibition Facilitates RNA-Mediated Reprogramming of Human Somatic Cells to Naive Pluripotency. *Stem Cell Reports* **13**, 1083–1098 (2019).
4. Castel, G. *et al.* Induction of Human Trophoblast Stem Cells from Somatic Cells and Pluripotent Stem Cells. *Cell Rep.* **33**, 108419 (2020).
5. Guo, G. *et al.* Human Naïve Epiblast Cells Possess Unrestricted Lineage Potential. doi:10.1101/2020.02.04.933812.
6. Yanagida, A. *et al.* Naive stem cell blastocyst model captures human embryo lineage segregation. *Cell Stem Cell* (2021) doi:10.1016/j.stem.2021.04.031.
7. Amita, M. *et al.* Complete and unidirectional conversion of human embryonic stem cells to trophoblast by BMP4. *Proc. Natl. Acad. Sci. U. S. A.* **110**, E1212–21 (2013).
8. Io, S. *et al.* Capturing human trophoblast development with naive pluripotent stem cells in vitro. *Cell Stem Cell* **28**, 1023–1039.e13 (2021).
9. Rivron, N. C. *et al.* Tissue deformation spatially modulates VEGF signaling and angiogenesis. *Proc. Natl. Acad. Sci. U. S. A.* **109**, 6886–6891 (2012).
10. Yu, F.-X. *et al.* Regulation of the Hippo-YAP pathway by G-protein-coupled receptor signaling. *Cell* **150**, 780–791 (2012).
11. Hardy, K., Handyside, A. H. & Winston, R. M. The human blastocyst: cell number, death and allocation during late preimplantation development in vitro. *Development* **107**, 597–604 (1989).
12. Niakan, K. K. & Eggan, K. Analysis of human embryos from zygote to blastocyst reveals distinct gene expression patterns relative to the mouse. *Dev. Biol.* **375**, 54–64 (2013).
13. Meistermann, D. *et al.* Integrated pseudotime analysis of human pre-implantation embryo single-cell transcriptomes reveals the dynamics of lineage specification. *Cell Stem Cell* (2021) doi:10.1016/j.stem.2021.04.027.
14. Lewis, W. H. & Gregory, P. W. CINEMATOGRAPHS OF LIVING DEVELOPING RABBIT-EGGS. *Science* **69**, 226–229 (1929).
15. Nichols, J. & Smith, A. Naive and primed pluripotent states. *Cell Stem Cell* **4**, 487–492 (2009).
16. Petropoulos, S. *et al.* Single-Cell RNA-Seq Reveals Lineage and X Chromosome Dynamics in Human Preimplantation Embryos. *Cell* vol. 167 285 (2016).
17. Zhou, F. *et al.* Reconstituting the transcriptome and DNA methylome landscapes of human implantation. *Nature* **572**, 660–664 (2019).
18. Tyser, R. C. V. *et al.* A spatially resolved single cell atlas of human gastrulation. *bioRxiv* (2020) doi:10.1101/2020.07.21.213512.
19. Zhao, C. *et al.* Reprogrammed iBlastoids contain amnion-like cells but not trophectoderm. doi:10.1101/2021.05.07.442980.
20. Messmer, T. *et al.* Transcriptional Heterogeneity in Naive and Primed Human Pluripotent Stem Cells at Single-Cell Resolution. *Cell Rep.* **26**, 815–824.e4 (2019).
21. Okae, H. *et al.* Derivation of Human Trophoblast Stem Cells. *Cell Stem Cell* **22**, 50–63.e6 (2018).
22. Mischler, A. *et al.* Two distinct trophectoderm lineage stem cells from human pluripotent stem cells. *J. Biol. Chem.* **296**, 100386 (2021).
23. Meistermann, D. *et al.* Spatio-temporal analysis of human preimplantation development reveals dynamics of epiblast and trophectoderm. doi:10.1101/604751.
24. Stirparo, G. G. *et al.* Integrated analysis of single-cell embryo data yields a unified transcriptome signature for the human pre-implantation epiblast. *Development* **145**, (2018).
25. Linneberg-Agerholm, M. *et al.* Naïve human pluripotent stem cells respond to Wnt, Nodal, and LIF signalling to produce expandable naïve extra-embryonic endoderm. *Development* (2019) doi:10.1242/dev.180620.

26. Guo, G. *et al.* Naive Pluripotent Stem Cells Derived Directly from Isolated Cells of the Human Inner Cell Mass. *Stem Cell Reports* **6**, 437–446 (2016).
27. Rivron, N. C. *et al.* Blastocyst-like structures generated solely from stem cells. *Nature* **557**, 106–111 (2018).
28. Maître, J.-L. *et al.* Asymmetric division of contractile domains couples cell positioning and fate specification. *Nature* **536**, 344–348 (2016).
29. Nishioka, N. *et al.* The Hippo signaling pathway components Lats and Yap pattern Tead4 activity to distinguish mouse trophectoderm from inner cell mass. *Dev. Cell* **16**, 398–410 (2009).
30. Gerri, C. *et al.* Initiation of a conserved trophectoderm program in human, cow and mouse embryos. *Nature* **587**, 443–447 (2020).
31. Zhao, B. *et al.* Inactivation of YAP oncoprotein by the Hippo pathway is involved in cell contact inhibition and tissue growth control. *Genes Dev.* **21**, 2747–2761 (2007).
32. Lin, K. C., Park, H. W. & Guan, K.-L. Regulation of the Hippo Pathway Transcription Factor TEAD. *Trends Biochem. Sci.* **42**, 862–872 (2017).
33. Wei, H. *et al.* Verteporfin suppresses cell survival, angiogenesis and vasculogenic mimicry of pancreatic ductal adenocarcinoma via disrupting the YAP-TEAD complex. *Cancer Sci.* **108**, 478–487 (2017).
34. Dumortier, J. G. *et al.* Hydraulic fracturing and active coarsening position the lumen of the mouse blastocyst. *Science* **365**, 465–468 (2019).
35. Aberkane, A. *et al.* Expression of adhesion and extracellular matrix genes in human blastocysts upon attachment in a 2D co-culture system. *MHR: Basic science of reproductive medicine* (2018) doi:10.1093/molehr/gay024.
36. Lindenberg, S. 1 Ultrastructure in human implantation: Transmission and scanning electron microscopy. *Baillière's Clinical Obstetrics and Gynaecology* vol. 5 1–14 (1991).
37. Boretto, M. *et al.* Development of organoids from mouse and human endometrium showing endometrial epithelium physiology and long-term expandability. *Development* **144**, 1775–1786 (2017).
38. Kelleher, A. M. *et al.* Integrative analysis of the forkhead box A2 (FOXA2) cistrome for the human endometrium. *FASEB J.* **33**, 8543–8554 (2019).
39. Massimiani, M. *et al.* Molecular Signaling Regulating Endometrium-Blastocyst Crosstalk. *Int. J. Mol. Sci.* **21**, (2019).
40. Wang, W. *et al.* Single-cell transcriptomic atlas of the human endometrium during the menstrual cycle. *Nat. Med.* **26**, 1644–1653 (2020).
41. Altmäe, S. *et al.* Meta-signature of human endometrial receptivity: a meta-analysis and validation study of transcriptomic biomarkers. *Sci. Rep.* **7**, 10077 (2017).
42. Bentin-Ley, U. *et al.* Ultrastructure of human blastocyst-endometrial interactions in vitro. *J. Reprod. Fertil.* **120**, 337–350 (2000).
43. Matsuo, M. *et al.* Levonorgestrel Inhibits Embryo Attachment by Eliminating Uterine Induction of Leukemia Inhibitory Factor. *Endocrinology* **161**, (2020).
44. Xu, S., Grande, F., Garofalo, A. & Neamati, N. Discovery of a novel orally active small-molecule gp130 inhibitor for the treatment of ovarian cancer. *Mol. Cancer Ther.* **12**, 937–949 (2013).
45. Triastuti, E. *et al.* Pharmacological inhibition of Hippo pathway, with the novel kinase inhibitor XMU-MP-1, protects the heart against adverse effects during pressure overload. *Br. J. Pharmacol.* **176**, 3956–3971 (2019).
46. Ma, H. *et al.* In vitro culture of cynomolgus monkey embryos beyond early gastrulation. *Science* **366**, (2019).
47. Xiang, L. *et al.* A developmental landscape of 3D-cultured human pre-gastrulation embryos. *Nature* **577**, 537–542 (2020).
48. Shakiba, N. *et al.* CD24 tracks divergent pluripotent states in mouse and human cells. *Nat. Commun.* **6**, 7329 (2015).
49. Zheng, Y. *et al.* Controlled modelling of human epiblast and amnion development using stem cells. *Nature* **573**, 421–425 (2019).
50. Hyun, I., Munsie, M., Pera, M. F., Rivron, N. C. & Rossant, J. Toward Guidelines for

Research on Human Embryo Models Formed from Stem Cells. *Stem Cell Reports* **14**, 169–174 (2020).
51. Gardner, D. K. & Schoolcraft, W. B. Culture and transfer of human blastocysts. *Curr. Opin. Obstet. Gynecol.* **11**, 307–311 (1999).
52. Jeschke, U. *et al.* The human endometrium expresses the glycoprotein mucin-1 and shows positive correlation for Thomsen-Friedenreich epitope expression and galectin-1 binding. *J. Histochem. Cytochem.* **57**, 871–881 (2009).
53. Zhang, Y. *et al.* Cellinker: a platform of ligand–receptor interactions for intercellular communication analysis. *Bioinformatics* (2021) doi:10.1093/bioinformatics/btab036.
54. Guo, G. *et al.* Epigenetic resetting of human pluripotency. *Development* **144**, 2748–2763 (2017).
55. Vrij, E. J. *et al.* 3D high throughput screening and profiling of embryoid bodies in thermoformed microwell plates. *Lab Chip* **16**, 734–742 (2016).
56. Turco, M. Y. *et al.* Trophoblast organoids as a model for maternal-fetal interactions during human placentation. *Nature* **564**, 263–267 (2018).
57. Kim, S.-I. *et al.* Inducible Transgene Expression in Human iPS Cells Using Versatile All-in-One piggyBac Transposons. *Methods Mol. Biol.* **1357**, 111–131 (2016).
58. Picelli, S. *et al.* Full-length RNA-seq from single cells using Smart-seq2. *Nat. Protoc.* **9**, 171–181 (2014).
59. Turco, M. Y. *et al.* Long-term, hormone-responsive organoid cultures of human endometrium in a chemically defined medium. *Nature Cell Biology* vol. 19 568–577 (2017).
60. Heijmans, J. *et al.* ER stress causes rapid loss of intestinal epithelial stemness through activation of the unfolded protein response. *Cell Rep.* **3**, 1128–1139 (2013).
61. Kimmelman, J. *et al.* New ISSCR guidelines: clinical translation of stem cell research. *Lancet* **387**, 1979–1981 (2016).
62. Gardner, D. K., Lane, M., Stevens, J., Schlenker, T. & Schoolcraft, W. B. Blastocyst score affects implantation and pregnancy outcome: towards a single blastocyst transfer. *Fertil. Steril.* **73**, 1155–1158 (2000).

Supplementary table 1: List of primary Antibodies

Antibody	Company	Catalog Number	Dilution
NANOG	Abcam	ab109250	1:100
CDX2	Emergo Europe	MU392A-5UC	1:100
GATA4	Invitrogen	14-9980-82	1:400
OCT4	Santacruz Biotechnology	sc-5279	1:100
GATA3	Santacruz Biotechnology	sc-9009	1:100
GATA3	Invitrogen	14-9966-82	1:200
ZO-1	Invitrogen	339100	1:100
CDH1	eBioscience	14-3249-82	1:250
aPKC	Santacruz Biotechnology	sc-216	1:100
CK7	Abcam	ab181598	1:300
KLF17	Sigma	HPA002926	1:200
YAP1	Santacruz Biotechnology	sc-101199	1:100
NR2F2	Abcam	ab211776	1:100
AQP3	ac on lines	ABIN863208	1:100
CGβ	Dako	A0231	1:300
CGβ	Abcam	ab9582	1:200
PAEP	Abclonal	A5751	1:500
FOXA2	Cell signal	8186	1:1000
Acetylated Tubulin	Sigma	T7451	1:500
GATA2	Abcam	ab109241	1:250
TROP2	R&D systems	MAB650	1:00 (IHC) 1:50 (FACS)
PDGFRα	R&D systems	AF307	1:00 (IHC) 1:50 (FACS)

SOX17	R&D systems	AF1924-SP	1:200
KLF4	Sigma	HPA002926	1:200
OTX2	R&D systems	AF1979	1:100
SUSD2	Miltenyibiotec	130-117-682	1:100
CCR7	Thermo scientific	MA5-31992	1:200
SOX2	Invitrogen	14-9811-80	1:200
MUC1	Invitrogen	MA1-35039	1:200
CD24	BD Biosciences	561644	1:100
PODXL	R&D systems	MAB1658	1:100
TFAP2C	R&D systems	AF5059	1:100

Supplementary table 2: qPCR primers:

Gene Symbol	Gene name	Forward primer	Reverse primer
DPP4	Dipeptidyl peptidase 4	TACAAAAGTGACATGCCTCAGTT	TGTGTAGAGTATAGAGGGGCAGA
SPP1	Secreted phosphoprotein 1	GGCTGATTCTGGAAGTTCTGAG	TACTTGGAAGGGTCTGTGGG
LIF	Leukemia inhibitory factor	ATTCTCTATTACACAGCCCAGG	TACACGACTATGCGGTACAG
GPX3	Glutathione peroxidase 3	CATTCGGTCTGGTCATTCTGG	GGAGGACAGGAGTTCTTTAGG
PAEP	Progestagen associated endometrial protein	GTTCAAGATCAACTATACGGTGG	GCTCTTCCATCTGTTTCAAGTC
ASCL2	Achaete-scute complex homolog 2	CACTGCTGGCAAACGGAGAC	AAAACTCCAGATAGTGGGGGC
MMP2	Matrix metalloproteinase-2	GGCACCCATTTACACCTACA	AACCGGTCCTTGAAGAAGAAG
ITGA5	Integrin Subunit Alpha 5	GCCTGTGGAGTACAAGTCCTT	AATTCGGGTGAAGTTATCTGTGG
CGB	Chorionic gonadotropin beta	TGTGCATCACCGTCAACA	TGCACATTGACAGCTGAGAG

CGA	Chorionic Gonadotropinalpha	CAGAATGCACGCTACAGGAA	CGTGTGGTTCTCCACTTTGA
CYP19H1	Cytochrome P450 Family 19 Subfamily A Member 1	ACTACAACCGGGTATATGGAGAA	TCGAGAGCTGTAATGATTGTGC